Testing sequence stratigraphic models by drilling Miocene foresets on the New Jersey shallow shelf

Kenneth G. Miller[1], Gregory S. Mountain[1], James V. Browning[1], Miriam E. Katz[2], Donald Monteverde[1], Peter J. Sugarman[1], Hisao Ando[3], Maria A. Bassetti[4], Christian J. Bjerrum[5], David Hodgson[6], Stephen Hesselbo[7], Sarp Karakaya[1], Jean-Noel Proust,[8] and Marina Rabineau[9]

[1]*Department of Earth and Planetary Sciences, Rutgers University, Piscataway, New Jersey 08854, USA*
[2]*Earth & Environmental Sciences, Rensselaer Polytechnic Institute, 1W08 JRSC, Troy, New York 12180, USA*
[3]*Department of Earth Sciences, Faculty of Science, Ibaraki University, Bunkyo 2-1-1, Mito 310-8512, Japan*
[4]*Laboratoire CEFREM Bat U, University of Perpignan, 52 Avenue Paul Alduy, Perpignan, 66860, France*
[5]*Department of Geography and Geology, University of Copenhagen, Øster Voldgade 10, DK-1350 København K, Denmark*
[6]*School of Earth and Environment, University of Leeds, Woodhouse Lane, Leeds LS2 9JT, UK*
[7]*Department of Earth Sciences, University of Oxford, South Parks Road, Oxford OX1 3AN, UK*
[8]*Géosciences, CNRS, Université Rennes, Campus de Beaulieu, 35042 Rennes, France*
[9]*UMR6538, Institut Universitaire Européen de La Mer Place Nicolas Copernic 29280 Plouzané, France*

ABSTRACT

We present seismic, core, log, and chronologic data on three early to middle Miocene sequences (m5.8, m5.4, and m5.2; ca. 20–14.6 Ma) sampled across a transect of seismic clinothems (prograding sigmoidal sequences) in topset, foreset, and bottomset locations beneath the New Jersey shallow continental shelf (Integrated Ocean Drilling Program Expedition 313, Sites M27–M29). We recognize stratal surfaces and systems tracts by integrating seismic stratigraphy, lithofacies successions, gamma logs, and foraminiferal paleodepth trends. Our interpretations of systems tracts, particularly in the foresets where the sequences are thickest, allow us to test sequence stratigraphic models. Landward of the clinoform rollover, topsets consist of nearshore deposits above merged transgressive surfaces (TS) and sequence boundaries overlain by deepening- and fining-upward transgressive systems tracts (TST) and coarsening- and shallowing-upward highstand systems tracts (HST). Drilling through the foresets yields thin (<18 m thick) lowstand systems tracts (LST), thin (<26 m) TST, and thick HST (15–90 m). This contrasts with previously published seismic stratigraphic predictions of thick LST and thin to absent TST. Both HST and LST show regressive patterns in the cores. Falling stage systems tracts (FSST) are tentatively recognized by seismic downstepping, although it is possible that these are truncated HST; in either case, these seismic geometries consist of uniform sands in the cores with a blocky gamma log pattern. Parasequence boundaries (flooding surfaces) are recognized in LST, TST, and HST. TS are recognized as an upsection change from coarsening- to fining-upward successions. We find little evidence for correlative conformities; even in the foresets, where sequences are thickest, there is evidence of erosion and hiatuses associated with sequence boundaries. Sequence m5.8 appears to be a single million-year-scale sequence, but sequence m5.4 is a composite of 3 ~100-k.y.-scale sequences. Sequence m5.2 may also be a composite sequence, although our resolution is insufficient to demonstrate this. We do not resolve the issue of fractal versus hierarchical order, but our data are consistent with arrangement into orders based on Milankovitch forcing on eccentricity (2.4 m.y., 405 and 100 k.y. cycles) and obliquity scales (1.2 m.y. and 41 k.y.).

INTRODUCTION

Sequence stratigraphy is based on recognition of unconformity-bounded sedimentary units on seismic profiles, in outcrop, in cored sections, and on geophysical logs (Vail et al., 1977; Van Wagoner et al., 1990). Sequences are objective units (e.g., Neal and Abreu, 2009), but the interpretation of sequences is often tied to genetic criteria (Mitchum et al., 1977), especially relative sea-level change. The genetic connotation remains controversial (e.g., Christie-Blick et al., 1988, 1990; Miall, 1991; Christie-Blick, 1991; Catuneanu, 2006; Embry, 2009). In addition, sequence nomenclature and approaches have proliferated, leading some to plead for a return to basics (Neal and Abreu, 2009). Basic principles of sequence stratigraphy focus on three stratal surfaces, i.e., sequence boundaries (SB), transgressive surfaces (TS), and maximum flooding surfaces (MFS), and stacking patterns of parasequences (those bounded by flooding surfaces) and the attendant trends observed in cores as deepening- and shallowing-upward successions (Fig. 1). They are not explicitly tied to a relative sea-level curve. We adopt a back to basics approach using new drilling data to address the architecture of seismic and core sequences.

A series of publications by Exxon Production Research Company illustrated sequences as sigmoidal, slug-shaped units with thin topsets, thick foresets, and thin bottomset deposits bounded by sigmoidal clinoformal unconformities and correlative conformities (Fig. 1; Vail, 1987; Van Wagoner et al., 1987; Posamentier and Vail, 1988; Posamentier et al., 1988). We apply the term clinothem to Miocene seismic sequences imaged beneath the New Jersey continental shelf (Figs. 2 and 3). Clinothems are packages of sediment that prograde seaward and are bounded by surfaces (in this case sequence boundaries) with distinct sigmoidal (clinoform) geometry. The clinothem topsets were originally termed as the shelf and the rollover point as the shelf break (Vail et al., 1977). This has created

Geosphere; October 2013; v. 9; no. 5; p. 1236–1256; doi:10.1130/GES00884.1; 13 figures; 7 supplemental figures.
Received 14 November 2012 ♦ Revision received 1 July 2013 ♦ Accepted 8 August 2013 ♦ Published online 13 September 2013

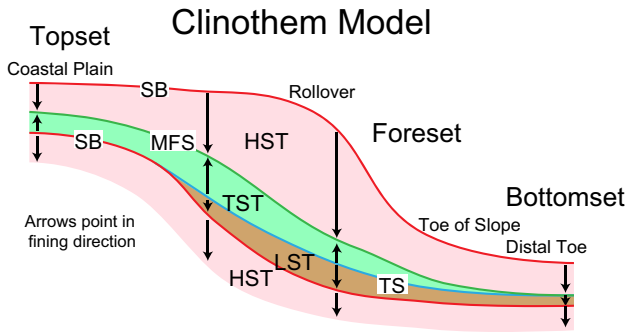

Figure 1. Clinothem model; arrows point in fining (deepening) direction. SB—sequence boundary (red lines); TS—transgressive surface (blue lines); MFS—maximum flooding surface (green lines); LST—lowstand systems tract (brown); TST—transgressive systems tracts (green); and HST—highstand systems tract (light pink). Rollover is equivalent to depositional shelf break of several authors.

confusion because the modern continental shelf-slope break is typically in 120–200 m of water, averaging 135 m off New Jersey (Heezen et al., 1959). Two-dimensional backstripping of the New Jersey margin showed that the structurally controlled continental shelf-slope break occurred in 100–300 m of water from the Late Cretaceous to Miocene ~60 km seaward of Integrated Ocean Drilling Program Expedition 313 Site M29 (Steckler et al., 1999; Mountain et al., 2010) and that the rollover features (also called depositional shelf breaks, a term we avoid because it evokes the modern shelf break) associated with Miocene clinoforms are shallower, different features than the continental shelf-slope break.

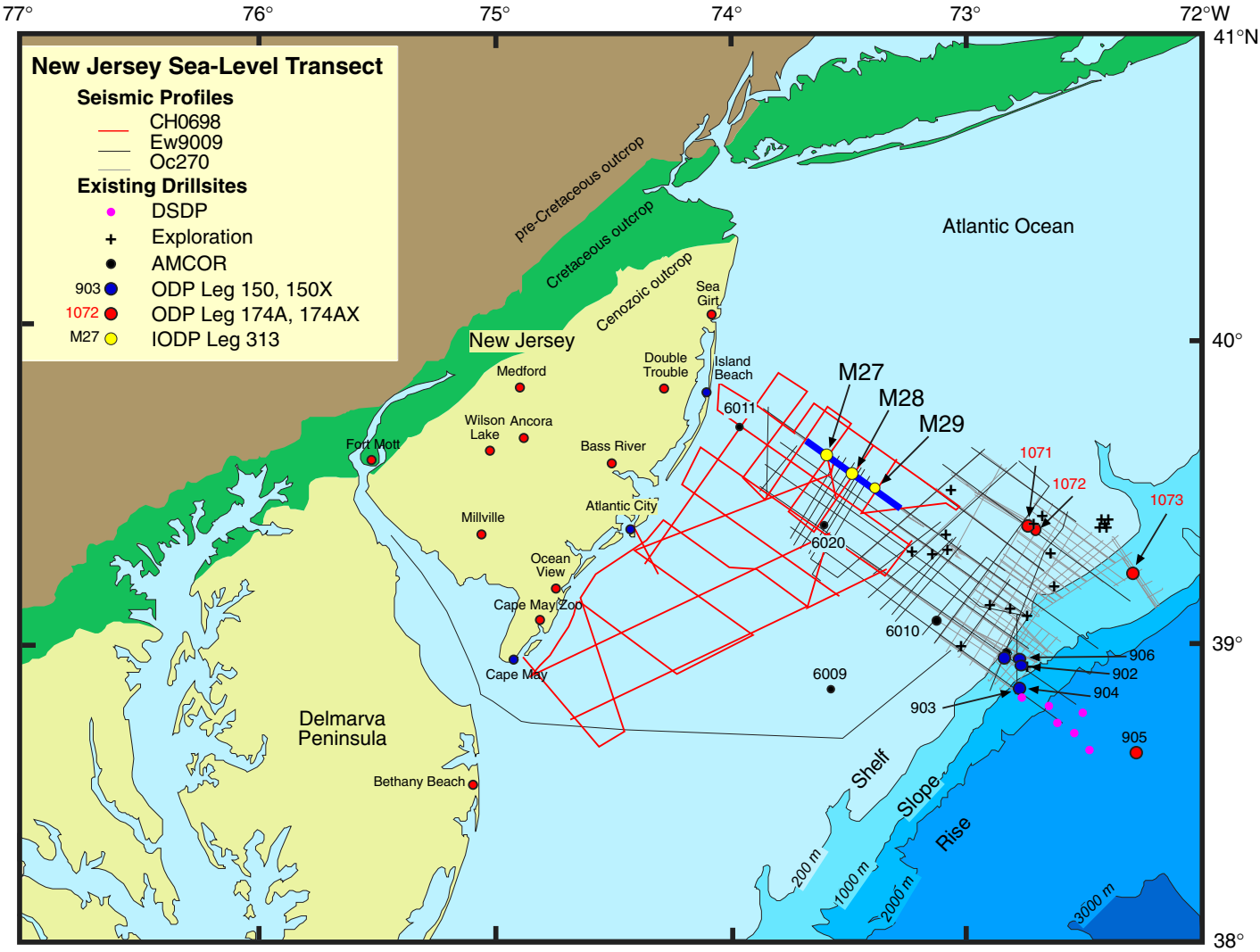

Figure 2. Generalized bathymetric location map of the New Jersey–Mid Atlantic Margin sea-level transect showing three generations of multichannel seismic data (cruises R/V *Ewing* Ew9009, R/V *Oceanus* Oc270, R/V *Cape Hatteras* CH0698), onshore coreholes, and offshore coreholes drilled by AMCOR (Atlantic Margin Coring Project; Hathaway et al., 1979), the Ocean Drilling Program (ODP), the Integrated Ocean Drilling Program (IODP), and the Deep Sea Drilling Project (DSDP).

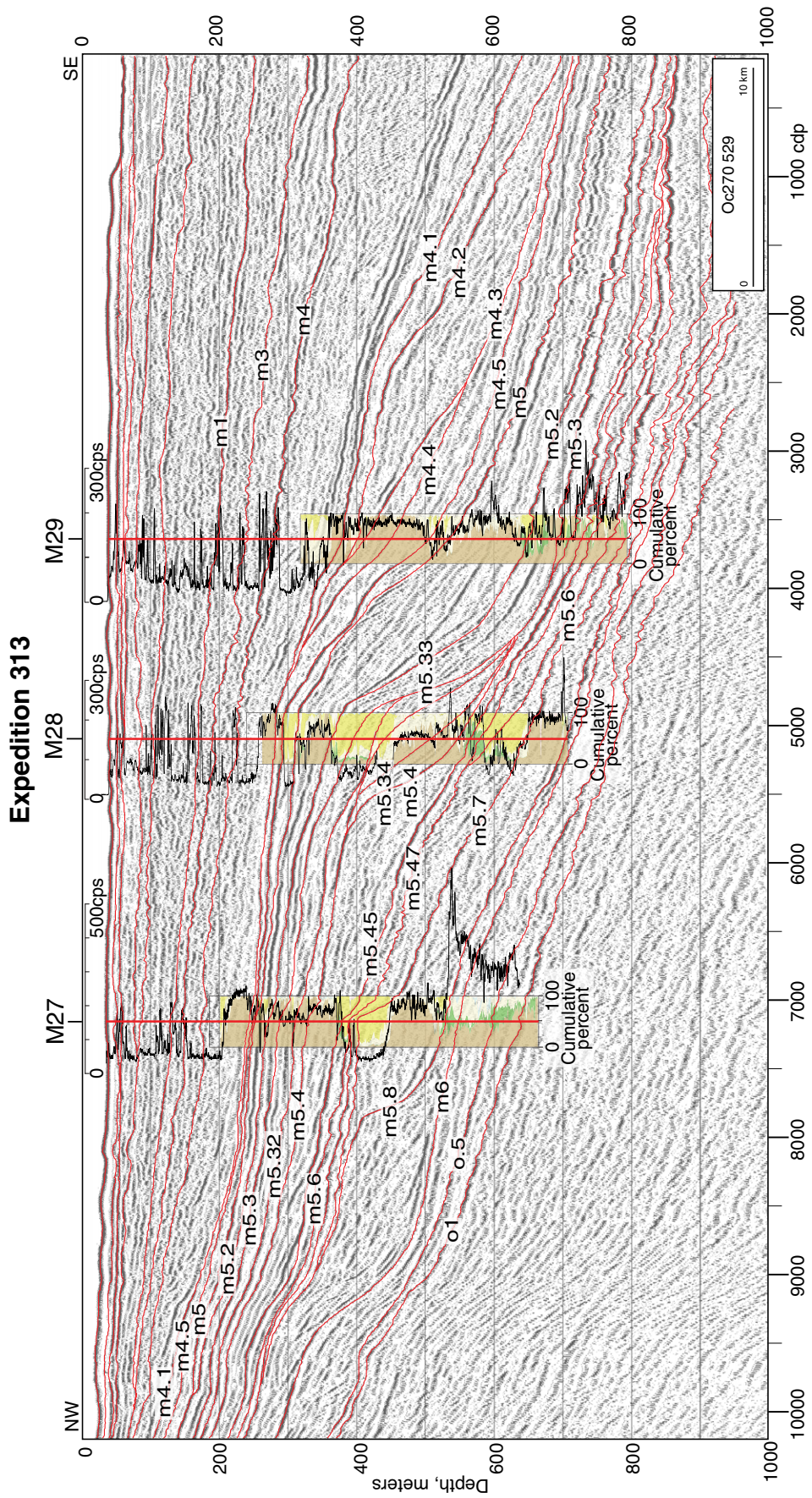

Figure 3. Multichannel seismic profile Oc270 529 (R/V *Oceanus*) in region of Integrated Ocean Drilling Program Expedition 313 providing a long dip profile from northwest (NW) to southeast (SE). Sites M27–M29 are located on this line. Axes are depth in meters obtained using the revised velocity-depth function (Mountain and Monteverde, 2012) and common depth points (1 cdp = 6.25 m); approximate scale (in km) is given on lower right. Major seismic sequence boundaries and select intrasequence reflectors (o1, o.5) are shown; all others are seismic sequence boundaries. Superimposed are the coarse fraction cumulative percent lithology and downhole gamma logs (in counts per second, cps) as described in Miller et al. (2013).

Subdivision of sequences into systems tracts has been explicitly tied to relative sea-level changes (Vail, 1987; Van Wagoner et al., 1987; Posamentier and Vail, 1988; Posamentier et al., 1988; Coe, 2003; Catuneanu, 2006) and interpretation of systems tracts is often needlessly highly model dependent. Systems tracts were defined as linked depositional systems (Brown and Fisher, 1977) that are used to subdivide sequences into lowstand systems tracts (LST), transgressive systems tracts (TST), and highstand systems tracts (HST; Vail, 1987; Van Wagoner et al., 1987; Posamentier and Vail, 1988; Posamentier et al., 1988). The falling stage systems tract (FSST) is a fourth systems tract (Plint and Nummedal, 2000), although its recognition can be controversial with respect to the location of the associated overlying sequence boundary (see summary in Coe, 2003). The LST, TST, and HST are separated by two distinct stratal surfaces: the transgressive surface (TS) and the maximum flooding surface (MFS). We summarize systems tracts as they apply to siliciclastic environments, focusing on these surfaces.

The fundamental surface in sequence stratigraphy is the sequence boundary and its recognition is of primary importance. Seismic stratigraphic criteria for the sequence boundary include onlap, downlap, toplap, and erosional truncation (Mitchum et al., 1977). Criteria from core observations include irregular contacts, rip-up clasts, other evidence of reworking, intense bioturbation, major facies changes, stacking pattern changes (e.g., changes in coarsening versus fining upward; Fig. 1) and evidence for hiatuses (Van Wagoner et al., 1987; Miller et al., 2013). Geophysical log criteria include recognition of stacking patterns, particularly of parasequences (those bounded by flooding surfaces, FS; Van Wagoner et al., 1987, 1990), and the association of large uphole gamma-log increases with sequence boundaries, although these also occur at MFS. Sequence-bounding unconformities often lose seismic stratigraphic expression when traced basinward and the term correlative conformity has been included in the definition of sequence as a surface traced from the unconformity to one that has "…no physical evidence of erosion or non-deposition and no significant hiatus…" (Mitchum et al., 1977, p. 206).

The TS generally separates the LST below from the TST above. Where no LST deposits are present (as is often the case on topsets; Fig. 1), or in seismic data where thin LST sediments are below seismic resolution, the TS merges with the sequence boundary. The TS marks a change from progradational to retrogradational seismic stratigraphic successions and a change in cores from coarsening-upward to fining-upward successions (Fig. 1) in shelf depositional environments (though these patterns may be complicated in the nearshore setting), and may appear as a shift from regressive sands below to finer grained muds above (Vail, 1987; Van Wagoner et al., 1987, 1988, 1990; Posamentier and Vail, 1988; Posamentier et al., 1988). The TS is diachronous and often linked to local erosion associated with marine ravinement as shoreface erosion cannibalizes former barrier island deposits (Demarest and Kraft, 1987).

The MFS separates the TST from the HST. The MFS is recognized in seismic sections as a downlap surface, an upsection change from retrogrational to progradational successions in seismic profiles and outcrops, and in cores as a change from fining-upward to coarsening-upward successions (Fig. 1) (Vail, 1987; Van Wagoner et al., 1987, 1988; Posamentier and Vail, 1988; Posamentier et al., 1988). In cores, sediments deposited along the MFS usually record the deepest water of a sequence; furthermore, these sediments are often associated with a condensed section recognized by intense bioturbation, in situ glauconite, phosphorite, abundant organic carbon, greater mud versus sand, planktonic microfossils, and in situ shells (Loutit et al., 1988; Kidwell, 1989, 1991). The TST is transgressive (generally fining upsection; Fig. 1) and thus is associated with retrogradational parasequence sets, generally stepping up onto the topsets of the previous sequence (Fig. 1). The HST is regressive, associated with aggradational to progradational and degradational parasequence sets (Neal and Abreu, 2009), downlaps on the MFS, and is generally overlain by the upper sequence boundary (Vail, 1987; Van Wagoner et al., 1987, 1988; Posamentier and Vail, 1988; Posamentier et al., 1988).

Interpretation of the LST is controversial because of the uncertainties in placement of its base versus the FSST (Coe, 2003), the varied facies it contains, and the fact that it is the one salient feature separating sequences from transgressive-regressive cycles (Christie-Blick and Driscoll, 1995; Catuneanu et al., 2009; Embry, 2009). Vail et al. (1977) first termed all strata that onlap seaward of the clinothem rollover (Fig. 1; his shelf break) as lowstand deposits. Subsequent studies have defined the LST in terms of sea-level curves (Vail, 1987; Van Wagoner et al., 1987, 1988; Posamentier and Vail, 1988; Posamentier et al., 1988; Coe, 2003), engendering debate. There is general agreement that sediments of the LST directly overlie the sequence boundary, are the lower regressive systems tract containing progradational to aggradational parasequence sets, and generally coarsen up to the TS (Vail, 1987; Van Wagoner et al., 1987; Posamentier et al., 1988; Coe, 2003; Neal and Abreu, 2009). However, there has been a tendency to attribute all coarse-grained sediments overlying a sequence boundary to those of the LST, even when unjustified (e.g., transgressive estuarine gravels interpreted as lowstand deposits; Christie-Blick and Driscoll, 1995).

In the FSST, strata not only prograde as they do in the underlying HST, they also step down into the basin (often with sharp-based sands) and offlap progressively seaward (Plint and Nummedal, 2000), with progradation and progressively steepening foresets (e.g., Proust et al., 2001). The FSST is partially equivalent to the forced regression of Posamentier et al. (1992) and contrasts with the HST, where strata progressively onlap landward (Plint and Nummedal, 2000). A distinct surface separating the FSST from the underlying HST may be lacking (Plint and Nummedal, 2000). However, in many cases there is a marine erosion surface–associated regression (Proust et al., 2001), especially associated with Pleistocene 100 k.y. sequences (e.g., Trincardi and Correggiari, 2000; Rabineau et al., 2005). In general, the sequence boundary is placed at the top of the FSST (Plint and Nummedal, 2000), although "...there is still some controversy as to where the sequence boundary should be placed" (Coe, 2003, p. 86).

Most sequence stratigraphic interpretations rely heavily on links to hypothetical relative sea-level curves (see summary in Catuneanu et al., 2009). Early models interpreted deposition of (1) the LST from the time of maximum rate of relative and/or eustatic fall (falling inflection point) associated with the sequence boundary to the beginning of the rise (Posamentier et al., 1988); (2) the TST from the beginning of the rise to about the time of the maximum rate of rise at the MFS (Galloway, 1989); and (3) the HST from the maximum rate of rise to the time of maximum rate of fall (Posamentier and Vail, 1988). Subsequent publications have developed strikingly different timings (i.e., with the LST lagging a quarter cycle and starting at the beginning of the rise, MFS late in the relative rise) of systems tracts relative to hypothetical sea-level curves (e.g., Coe, 2003; Catuneanu et al., 2009; http://www.sepmstrata.org/page.aspx?&pageid=32&3). However, application of any model is an oversimplification because position of a stratal surface relative to a sea-level curve is a function of preexisting geometry, rates of subsidence (including differential subsidence that precludes computation of a single relative sea-level curve), and sedi-

ment supply (including shifting depocenters) (Christie-Blick et al., 1990).

The controversial nature of the LST (Christie-Blick, 1991; Christie-Blick and Driscoll, 1995) and the FSST (see summary in Coe, 2003) have led some to return to interpreting sequences as largely transgressive-regressive (T-R) cycles (Embry, 2009). T-R cycles describe sequences where lowstand deposits are absent, including many outcrop sections. For example, T-R cycles typify onshore New Jersey coastal plain deposition (e.g., Owens and Gohn, 1985), where the TS and sequence boundary are generally merged (Olsson et al., 1987; Sugarman et al., 1993; Miller et al., 1998). Similar T-R cycles have been interpreted in Europe (e.g., Hancock, 1993) and the western interior of the U.S. (e.g., Hancock and Kauffman, 1979). However, thin (<1 m) regressive LST can be preserved even on clinothem topsets of the New Jersey coastal plain (Miller et al., 1998; Browning et al., 2008), and geometries of forced regression, FSST, and lowstand deposits must be considered on the clinothem foresets. On the foresets, it is not an option to rely solely on T-R cycles, because lowstand deposits occur above sequence boundaries (Fig. 1).

Neal and Abreu (2009) focused on the basic stratal surfaces (SB, TS, and MFS) and stacking patterns of parasequence sets, following Mitchum and Van Wagoner (1991) in noting that sequences are scale independent. They identified systems tracts by distinguishing the following stacking patterns in cores and outcrop. (1) LST are progradational to aggradational (coarsening upward, ending in largely structureless sand; Fig. 1). (2) TST are retrogradational (fining upward; Fig. 1). (3) HST are aggradational to progradational and degradational (coarsening upward). Neal and Abreu (2009) noted that LST may be found landward of the rollover (depositional shelf edge). We adopt their approach of focusing on SB, TS, MFS and stacking and/or water depth trends using seismic-core-well log integration offshore of New Jersey.

The New Jersey margin has several generations of multichannel seismic data (MCS) that have imaged clinothem sequences (first called prograding deltas; Schlee, 1981). Greenlee et al. (1988) and Greenlee and Moore (1988) used industry seismic profiles to showcase the New Jersey shelf as a classic example of Miocene prograding sequences. Greenlee et al. (1992) interpreted the presence of thick lowstand wedges and HST, seismically lacking TST, for Miocene sequences beneath the middle to outer continental shelf of New Jersey. Poulsen et al. (1998) investigated middle Miocene sequences imaged in higher resolution seismic across the New Jersey outer continental shelf and reached a similar interpretation of only LST and HST. Monteverde et al. (2008) and Monteverde (2008) focused on Miocene sequences discussed here (ca. 23–13 Ma) that are landward of the middle to outer shelf seismic profiles of Greenlee et al. (1988) and Poulsen et al. (1998), and similarly concluded that sequences were almost approximately equal thicknesses of LST and HST, and that TST was either below seismic resolution or completely absent. The early to early-middle Miocene seismic sequences (discussed in Monteverde et al., 2008; Monteverde, 2008) were sampled by Integrated Ocean Drilling Program (IODP) Expedition 313 (Figs. 2 and 3; Supplemental Fig. 1[1]), with continuous cores and geophysical logs.

IODP Expedition 313 was designed to test sequence stratigraphic relationships across a series of early to middle Miocene clinothems (Figs. 2 and 3; Mountain et al., 2010); 15 early to middle Miocene (ca. 23–13 Ma) seismic sequence boundaries were recognized using criteria of onlap, downlap, erosional truncation, and toplap (Monteverde et al., 2008; Monteverde, 2008; Mountain et al., 2010). Core recovery was very good (~80%) considering the challenges in coring shallow-water sands and geophysical logs were obtained at all three sites. Sequence boundaries in cores and logs were recognized based on integrated study of key core surfaces, lithostratigraphy and process sedimentology (grain size, mineralogy, facies, and paleoenvironments), facies successions, benthic foraminiferal water depths, downhole logs, core gamma logs, and chronostratigraphic ages (Mountain et al., 2010; Miller et al., 2013). Velocity and density logs allow construction of synthetic seismograms at Sites M27 and M29 (Mountain and Monteverde, 2012), providing firm placement of sequence boundaries (Miller et al., 2013) and a starting point for deciphering systems tracts. Ages of sequences and hiatuses are derived by integrating Sr isotope stratigraphy and biostratigraphy (diatoms, nannofossils, and dinocysts) on age-depth diagrams with a resolution of ±0.25 to ±0.5 m.y. (Browning et al., 2013). In this contribution we focus on three sequences sampled across of full range of topset, foreset, and bottomsets: sequences m5.8, m5.4, and m5.2.

The objective of this paper is to integrate seismic interpretations done before drilling (Greenlee et al., 1988, 1992; Monteverde et al., 2008; Monteverde, 2008) with those done subsequently (Mountain et al., 2010; this study) and with core and geophysical log data to provide new insights into the interpretations of systems tracts focusing on critical thick foreset deposits (Figs. 4–11). We recognize stratal surfaces and systems tracts by integrating seismic stratigraphic interpretation, lithofacies successions, gamma logs, and benthic foraminiferal paleodepth trends. Our interpretation of systems tracts across the three clinothems allows us to test sequence stratigraphic models.

METHODS

Seismic Interpretation

Seismic sequence boundaries m5.8, m5.4, and m5.2 were identified in multichannel seismic grids obtained on R/V *Ewing* cruise Ew9009, R/V *Oceanus* cruise Oc270, and R/V *Cape Hatteras* cruise CH0698 (in 1990, 1995, and 1998, respectively; Monteverde et al., 2008; Monteverde, 2008; Mountain et al., 2010). We focus here on interpretations of Oc270 line 529, which crosses Sites M27, M28, and M29 (Figs. 2 and 3; Supplemental Fig. 1 [see footnote 1]). Seismic sequence boundaries m5.8, m5.4, and m5.2 were identified based on reflector terminations (onlap, downlap, erosional truncation, and toplap) on multiple lines and loop correlated throughout the seismic grids (Fig. 2). These criteria allow differentiation of these sequence boundaries from surfaces associated with FSST or truncated HST (e.g., reflectors 2 and 3 in Fig. 7). Sequences are named according to their basal reflector boundary, such that reflector m5.8 is the base of sequence m5.8. Several additional reflectors that are potential sequence boundaries (m5.34, m5.33, and m5.32; Fig. 3) were identified within sequence m5.4 (Fig. 3) by two of us (D. Monteverde and G. Mountain, *in* Mountain et al., 2010), but not loop correlated; their stratal significance is discussed herein. We trace internal reflectors within sequences m5.8, m5.4, and m5.2. MFS (green lines, Figs. 4–11) are seismically recognized by significant downlap across the sequence and onlap near to or landward of the rollover (Fig. 1); in sequences where there is more than one downlap surface, the stratigraphically lowest is taken as the seismic MFS. Seismic criteria alone are insufficient to unequivocally recognize TS, and placement of TS was done by iteration with core studies (see following). In all three cases, TS (blue lines, Figs. 4–11) onlap the basal sequence boundary seaward of the rollover and farther seaward downlap onto the sequence boundary or merge

[1]Supplemental Figure 1. (A) Uninterpreted MCS profile Oc270 Line 529 sized to print at 18 × 36 inches. (B) Interpreted MCS profile Oc270 Line 529 sized to print at 18 × 36 inches. If you are viewing the PDF of this paper or reading it offline, please visit http://dx.doi.org/10.1130/GES00884.S1 or the full-text article on www.gsapubs.org to view Supplemental Figure 1.

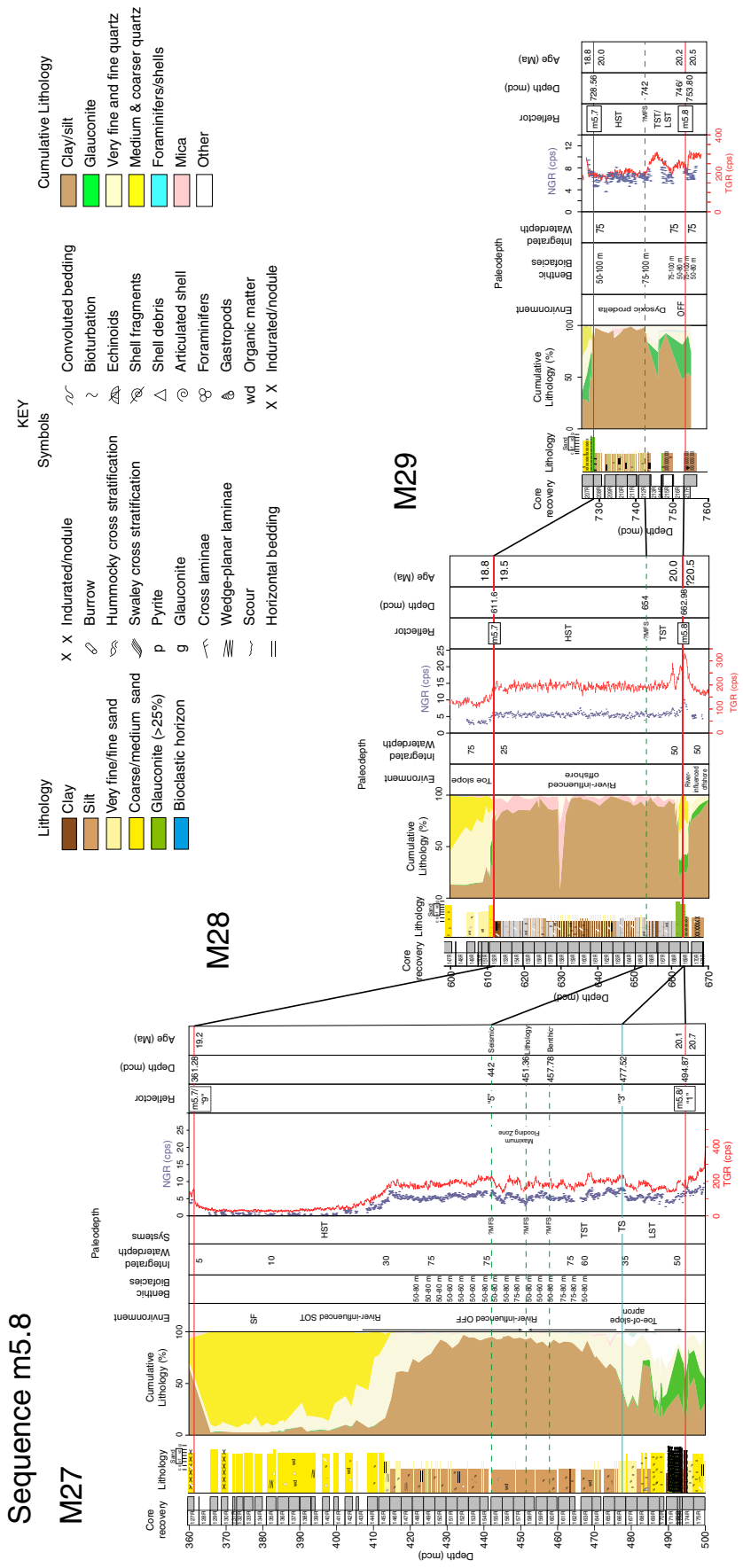

Figure 4. Comparison of sequence m5.8 at Integrated Ocean Drilling Program Expedition 313 Sites M27, M28, and M29, showing core depths in meters composite depth (mcd), core number (1H–21H, where H indicates recovery by hydraulic piston coring; R—rotary; and X—extended core barrel); core recovery (gray—recovered, white—gap); lithology (c—clay; s—silt; vf—very fine sand; vc—very coarse sand; g—gravel and/or pebbles); coarse fraction cumulative percent lithology (brown—mud; light yellow—fine quartz sand; dark yellow—medium-coarse quartz sand; green—glauconite sand; blue—carbonate [shells and foraminifera]; arrows point in fining direction); symbols on key at upper right (after Mountain et al., 2010). Environmental interpretation based on lithofacies is after Mountain et al. (2010) (SF—shoreface; SOT—shoreface-offshore transition [lower shoreface]; OFF—offshore). Paleowater depths (in meters) are based on benthic foraminiferal biofacies after Katz et al. (2013). Integrated paleowater depths (in meters) are based on benthic foraminiferal biofacies and lithofacies after Miller et al. (2013). Gamma logs: red—downhole wireline measurements as total gamma ray (TGR) in counts per second (cps); blue dots—natural gamma-ray (NGR) measurements made on unsplit whole cores, scale in cps; data after Mountain et al. (2010). Reflectors: red—sequence boundary; blue—transgressive surface (TS); green—maximum flooding surface (MFS). Dashed red lines—uncertain placement of sequence boundary. LST—lowstand systems tract; TST—transgressive systems tract; HST—highstand systems tract; FSST—falling stage systems tract. Ages for surface immediately below and above sequence boundaries are after Browning et al. (2013).

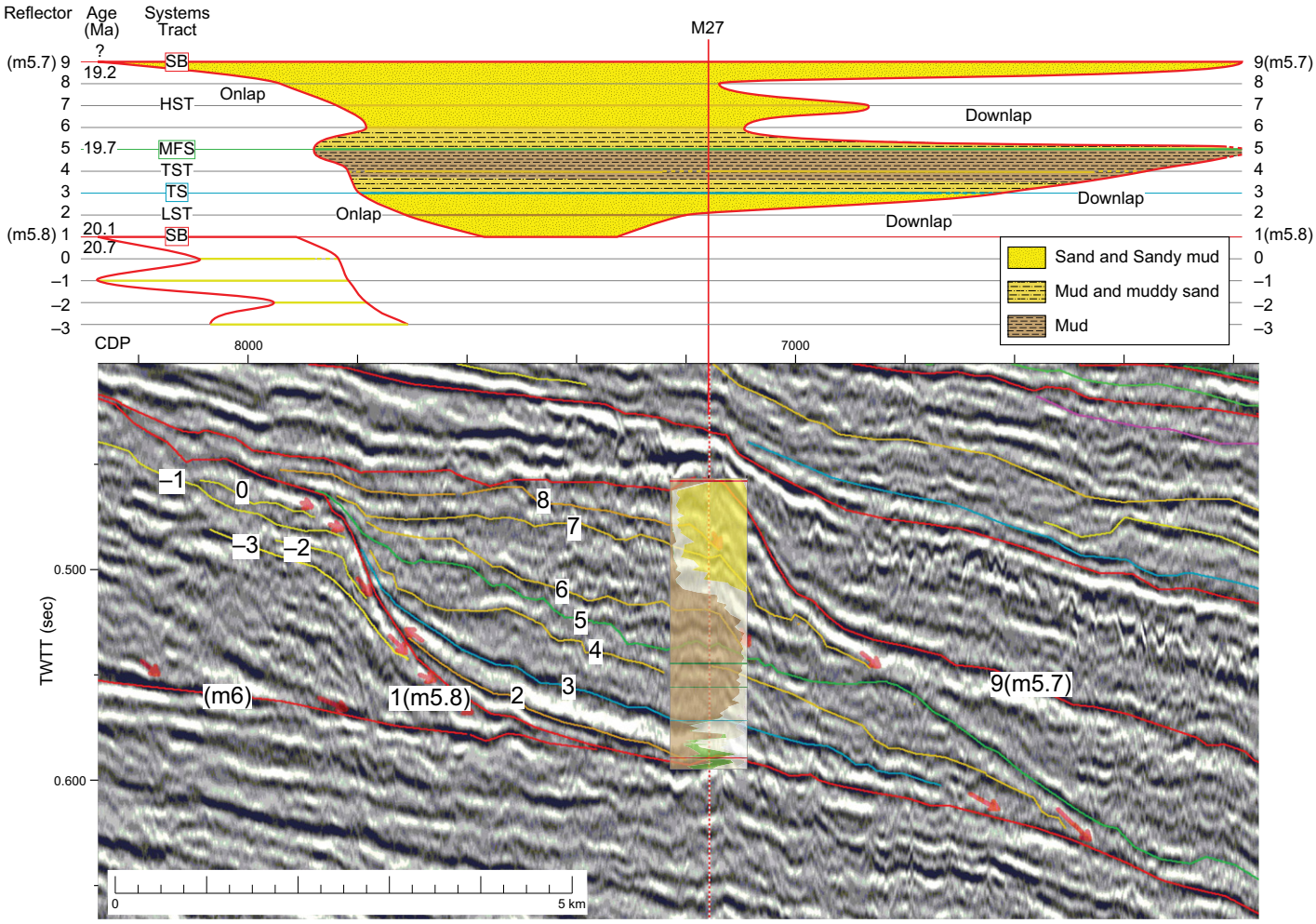

Figure 5. Interpreted seismic profile and Wheeler diagram (stratigraphic position versus distance; Wheeler, 1958) of sequence m5.8 across the foreset at Integrated Ocean Drilling Program Expedition 313 Site M27. Bottom panel is interpreted seismic profile in two-way traveltime (TWTT, in seconds versus cdp, common depth point). LST—lowstand systems tract; TST—transgressive systems tract; HST—highstand systems tract; FSST—falling stage systems tract; MFS—maximum flooding surface; SB—sequence boundary. Red arrows indicate reflector terminations; reflectors in red indicate sequence boundaries; reflectors in blue indicate TS; and reflectors in green indicate MFS. Other internal reflections are indicated in shades of yellow. Cumulative lithology is superimposed on the site. Arbitrary numbers assigned to reflectors are used to construct a time-distance plot at the top; scale of the Wheeler diagram on left assumes constant ages between reflectors; age estimates (shown in Ma) are derived from Browning et al. (2013).

with the MFS. Other internal reflections were traced (yellow lines, Figs. 5, 7, and 10) and used to interpret stacking patterns and to construct age-distance plots (top panels of Figs. 5, 7, and 10; also called Wheeler diagrams or chronostratigraphic charts of Vail et al., 1977).

Sequences, Lithology, and Paleoenvironments in Cores and Core-Seismic Integration

Sequence boundaries in the Expedition 313 cores were recognized on the basis of physical stratigraphy and age breaks (Mountain et al., 2010; Miller et al., 2013). Criteria for recognizing sequence-bounding unconformities in coreholes (e.g., Browning et al., 2006) that were applied to Expedition 313 cores include: (1) irregular contacts, with as much as 5 cm of relief on a 6.2-cm-diameter core; (2) reworking, including rip-up clasts found above the contact; (3) intense bioturbation, including burrows filled with overlying material; (4) major lithofacies shifts and changes in stacking pattern (discussed in the following); (5) upsection gamma-ray increases associated with changes from low-radioactivity sands below to hotter clays or glauconite sands immediately above sequence boundaries, and/or marine omission surfaces (e.g., with high U/Th scavenging); (6) shell lags above the contact; and (7) age breaks indicated by Sr isotope stratigraphy or biostratigraphy. Numerous sequence boundaries are illustrated in core photographs (Miller et al., 2013). A velocity versus depth function was used to make initial seismic-core correlations of seismic sequence boundaries to core surfaces identified from visual evidence (core descriptions and photographs) and log data (Mountain et al., 2010; Mountain and Monteverde, 2012; Miller et al., 2013). Synthetic seismograms from Sites M27A and M29A (Mountain and Monteverde, 2012) provide a check on seismic-core correlations and predicted depths of seismic sequence boundaries. The resultant seismic-core-log correlations (summarized in Miller et al., 2013) were used to construct site to site correlations for the three sequences m5.8, m5.4, and m5.2 that

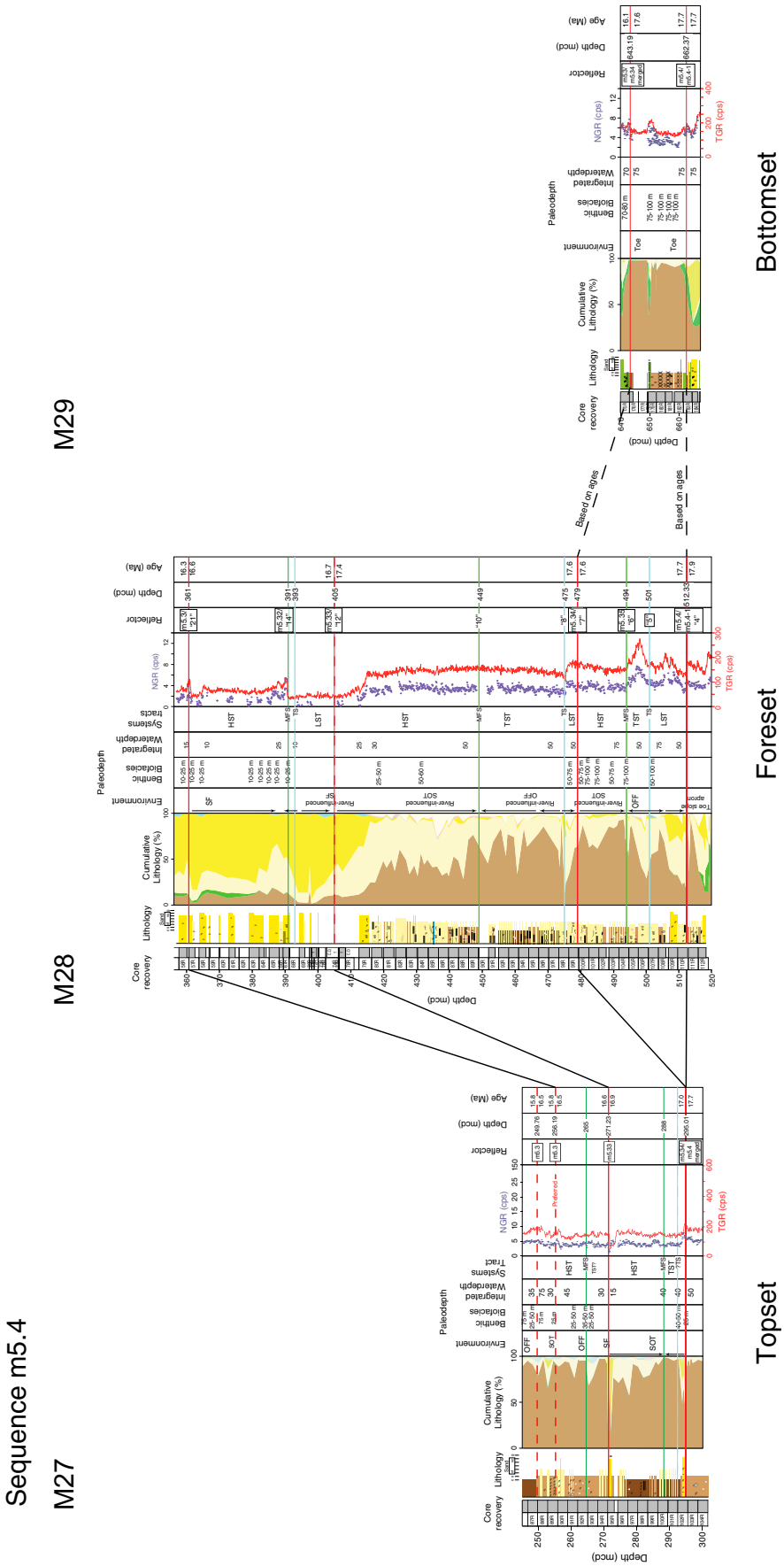

Figure 6. Comparison of sequence m5.4 at Integrated Ocean Drilling Program Expedition 313 Sites M27, M28, and M29. Caption and key as in Figure 4.

sampled topsets, foresets, and bottomsets in the three coreholes (Figs. 4, 6, and 9).

Lithologic trends are essential in interpreting systems tracts. The Expedition 313 sedimentologists produced visual core descriptions and differentiated clay, silt, and various sand fractions visually and using smear slides (Mountain et al., 2010). These lithologic descriptions have been synthesized into general lithology columns (essentially unchanged from Mountain et al., 2010) and presented as lithology in Figures 4, 6, and 8. Quantitative and qualitative lithology data were added (Miller et al., 2013) and weight percent mud (<63 µm), very fine and fine sand (63–250 µm), and medium sand and coarser sediment (>250 µm) were measured in washed samples at ~1.5 m intervals; the abundance of glauconite, shells, and mica in the sand fraction (>63 µm) was semiquantitatively determined by splitting 1727 samples into aliquots and visually estimating percentages on a picking tray. The data (presented as cumulative lithology in Figs. 4, 6, and 9) clearly show distinct trends in grain size and mineralogy that complement and extend the lithology columns presented as visual core descriptions (in Mountain et al., 2010).

Paleoenvironments are interpreted from lithofacies and biofacies. Lithofacies successions are interpreted using a wave-dominated shoreline model (summarized in Mountain et al., 2010), recognizing upper shoreface (0–5 m water depth), lower shoreface (5–10 m), shoreface-offshore transition (10–20 m), and offshore (>30 m) environments. Other environmental information (e.g., river-dominated) are from Mountain et al. (2010). Benthic foraminiferal biofacies were reported in Mountain et al. (2010) and in greater detail in Katz et al. (2013). Benthic foraminifera provide paleodepth constraints following the general paleobathymetric model of Miller et al. (1997) for coeval onshore New Jersey sections. In general, innermost neritic (<10 m) sediments were barren or yielded only *Lenticulina* spp., *Hanzawaia hughesi*–dominated biofacies are 10–25 m, *Nonionella pizarrensis*–dominated biofacies are 25–50 m, *Bulimina gracilis*–dominated biofacies are 50–80 m, *Uvigerina* spp.-dominated biofacies are 75–100 m, and high-diversity, low-dominance assemblages with key indicator taxa (e.g., *Cibicidoides pachyderma*, *Hanzawaia mantaensis*, and *Oridorsalis*) are >100 m (Mountain et al., 2010; Katz et al., 2013). In addition, planktonic foraminiferal abundance changes provide an additional proxy for water-depth variations at the Expedition 313 sites, with increasing percentages of planktonic foraminifera of total foraminifera with increasing water depth (Katz et al., 2013). We present both benthic forami-

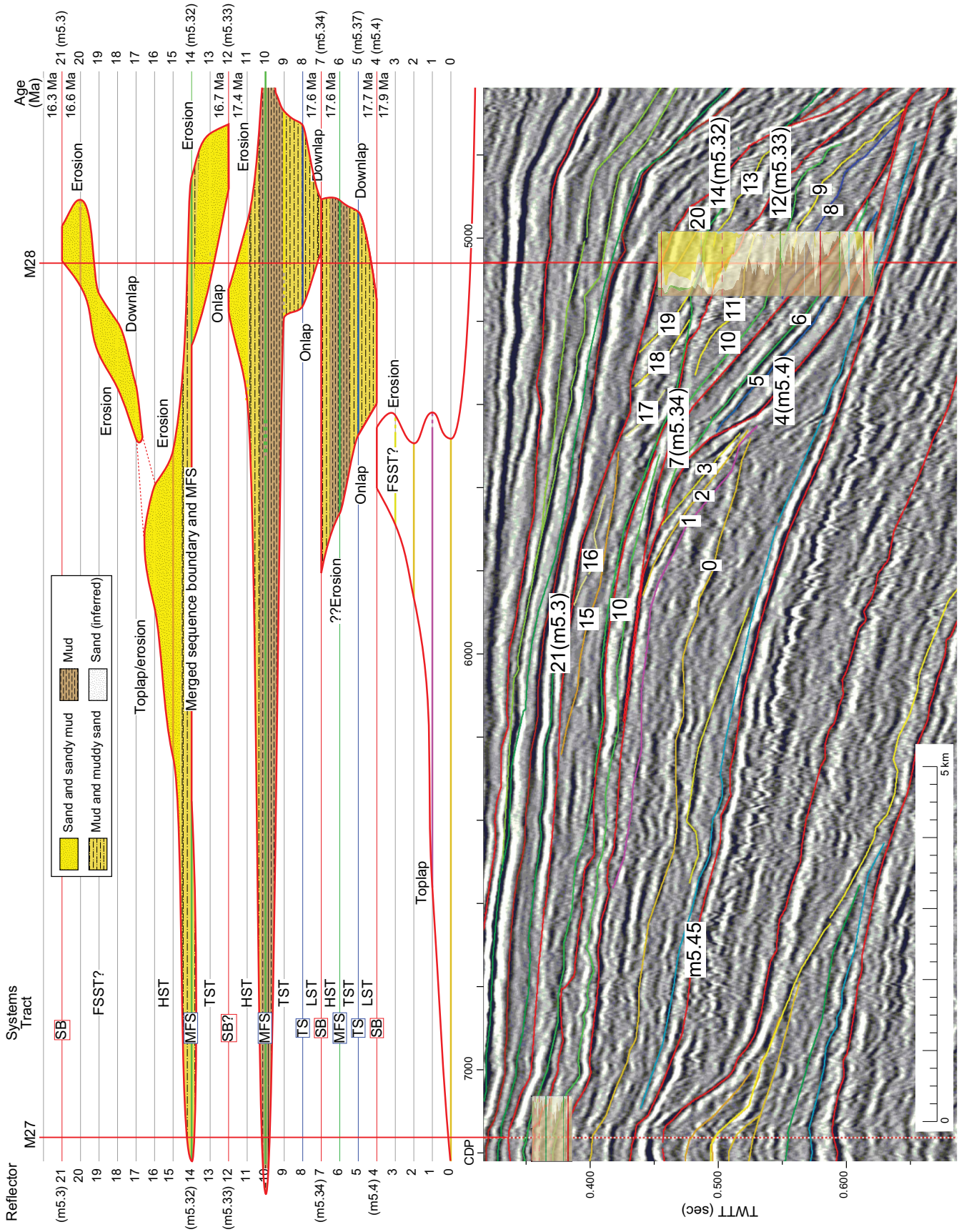

Figure 7. Interpreted seismic profile and Wheeler diagram of sequence m5.4 across the foreset at Integrated Ocean Drilling Program Expedition 313 Site M28, extending to the topset at Site M27. Caption as in Figure 5.

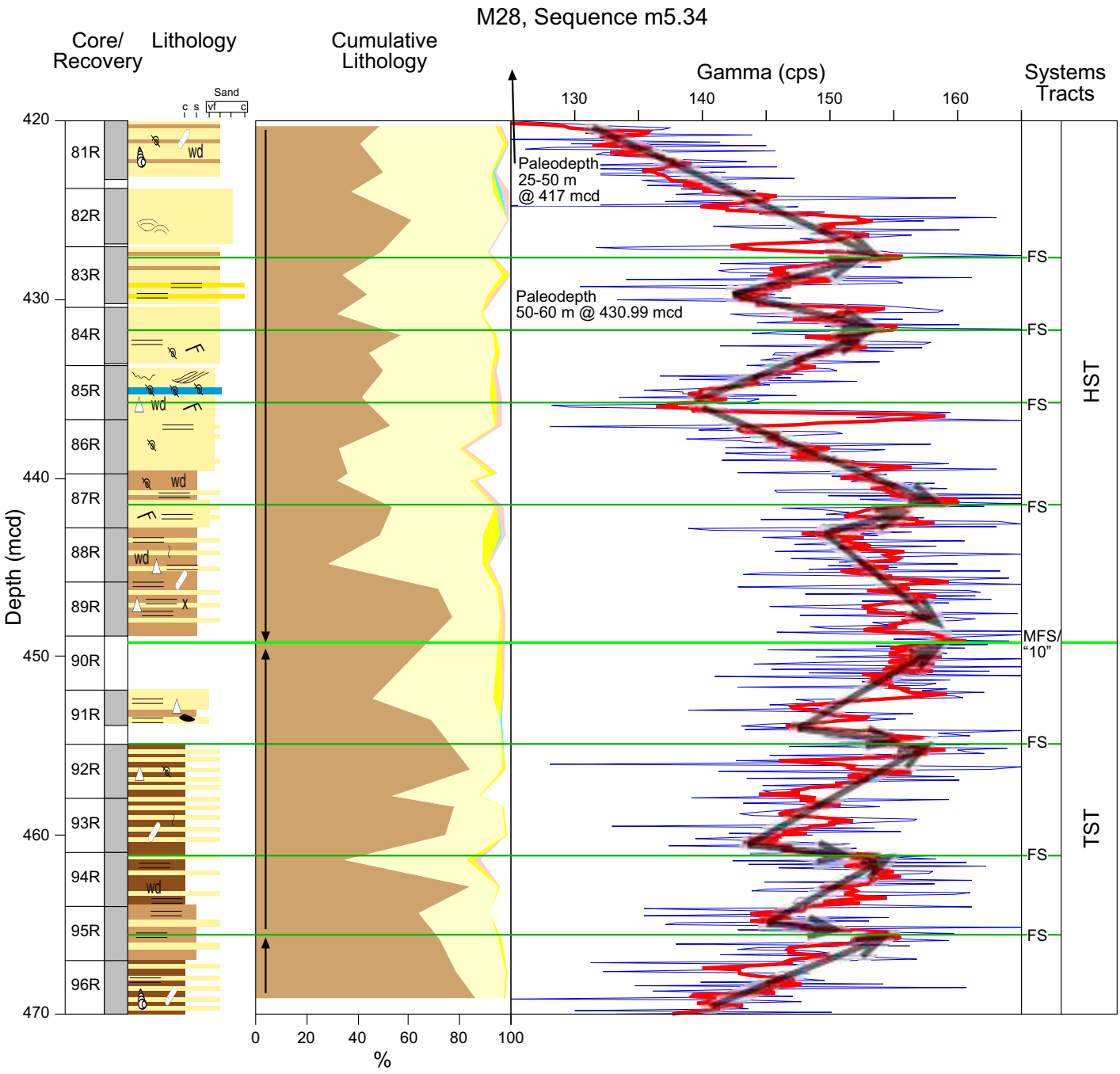

Figure 8. Enlargement of the upper part of the transgressive systems tract (TST) and lower highstand systems tract (HST) of the m5.34 sequence at Integrated Ocean Drilling Program Expedition 313 Site M28. Cumulative lithology and lithology columns as in Figure 6; caption and key as in Figure 4. The gamma log (thin purple line) has been smoothed with a 0.5 m filter (red line). Arrows point in inferred fining direction. Seven flooding sequences (FS; parasequence boundaries) and a maximum flooding surface (MFS) are inferred by the converging arrows.

niferal paleodepths and integrated paleodepths obtained by combining lithofacies and biofacies constraints (Figs. 4, 6, and 9) and percent planktonic foraminiferal data.

We present gamma-log values obtained downhole through the drill pipe (total gamma ray, TGR) and those obtained directly on the core in the laboratory (natural gamma ray, NGR) (Figs. 4, 6, and 9). Gamma-log data record lithologic variations primarily of quartz sands versus clays or glauconite-rich sediments, with low gamma readings in sands and high gamma-log values in muds, and generally highest values in glauconite-rich sediments.

Here we interpret TS, MFS, and systems tracts in sequences identified by Mountain et al. (2010) and updated in Miller et al. (2013, including detailed justification of placement of sequence boundaries). In cores, MFS are recognized by an uphole change in pattern from deepening-upward (generally fining upward)

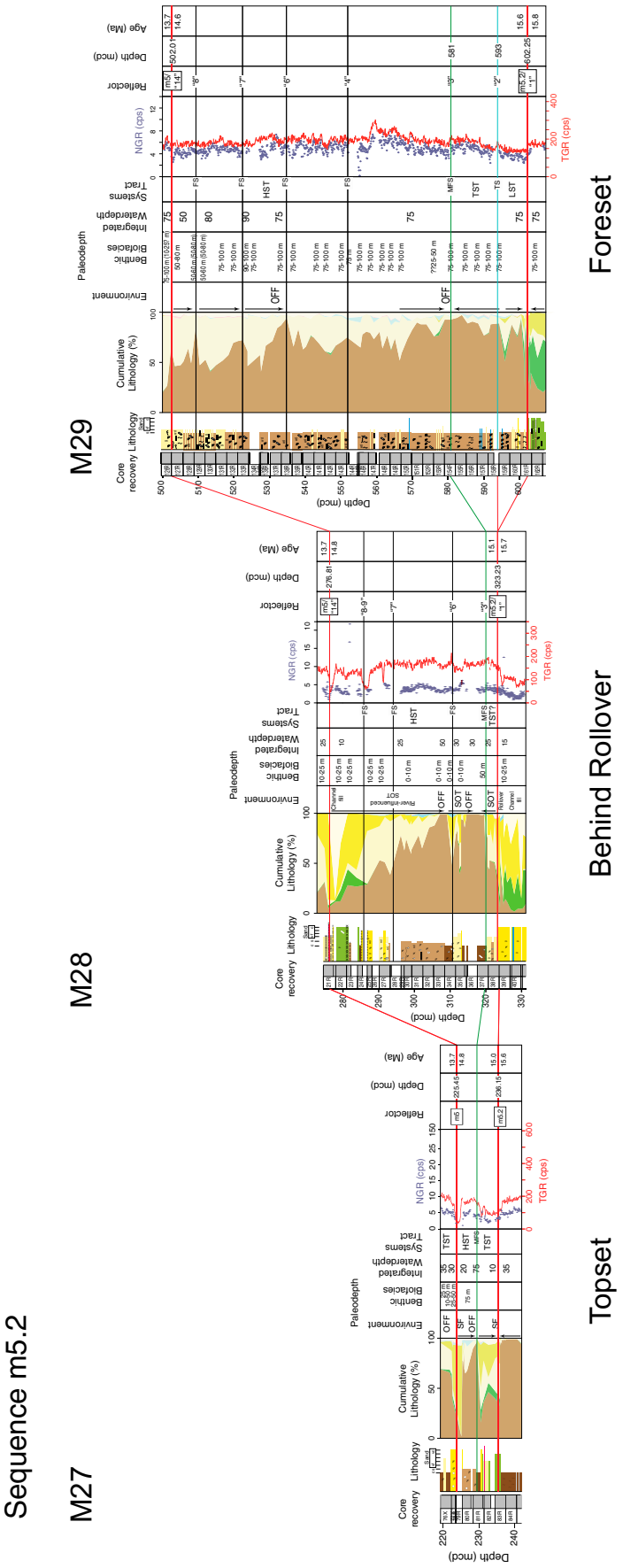

Figure 9. Comparison of sequence m5.2 at Integrated Ocean Drilling Program Expedition 313 Sites M27, M28, and M29. Caption as in Figure 4. Placement of internal reflectors 4–8 in the core is uncertain.

to shallowing-upward (generally coarsening upward) facies (Fig. 1) that is recognized using both lithologic and benthic foraminiferal criteria. MFS are associated with benthic foraminiferal evidence for deepening upsection to maximum water depths (typically associated with peaks in percent planktonic of total foraminifera; Loutit et al., 1988) and finest grain sizes. Both HST and LST show shallowing-upward successions inferred from coarsening-upward sections and benthic foraminiferal evidence. Transgressive surfaces are generally recognized by a change in stacking pattern from coarsening to fining upward (Fig. 1); they are often merged with sequence boundaries on the topsets. TST are transgressive (generally fining upward). Parasequence boundaries (flooding surfaces) are recognized in LST, TST, and HST by local peaks of percent mud and gamma-ray log stacking patterns. We do not identify systems tracts on the bottomsets due to the difficulty of resolving their complex stratal relationships with the data presented here (Mountain et al., 2010).

RESULTS

Sequence m5.8

Reflector m5.8 is clearly a seismic sequence boundary, based on onlap, toplap, erosional truncation, and downlap on line 529 (Figs. 3–5; Supplemental Figs. 2[2] and 3[3]) and elsewhere in the seismic grids (Monteverde et al., 2008; Monteverde, 2008). A possible FSST underlies the m5.8 seismic sequence boundary at common depth point (cdp) 7900–8100, where there are hints that reflectors (–2 and 0 in Fig. 5) step down into the basin (offlap). The overlying m5.7 sequence boundary extensively truncates the topset of the m5.8 sequence landward of Site M27, and the m5.8 sequence is completely eroded ~10 km landward of the site on Line 529. Sequence m5.8 was sampled in the foreset

[2]Supplemental Figure 2. Enlargement of Figure 4. If you are viewing the PDF of this paper or reading it offline, please visit http://dx.doi.org/10.1130/GES00884.S2 or the full-text article on www.gsapubs.org to view Supplemental Figure 2.

[3]Supplemental Figure 3. Uninterpreted (top) and interpreted (bottom) seismic profile *Oc270* Line 529 highlighting the m5.8 sequence. Scales are two-way travel-time (TWTT) in seconds and Common Depth Point. Approximate scale in km is given. Dotted line indicates location of Site M27. Arrows indicate reflector termination. Red are sequence boundaries, blue are transgressive surfaces, green are maximum flooding surfaces, and shades of yellow are other reflectors. Numbers (–3 to 8) are arbitrary designations. If you are viewing the PDF of this paper or reading it offline, please visit http://dx.doi.org/10.1130/GES00884.S3 or the full-text article on www.gsapubs.org to view Supplemental Figure 3.

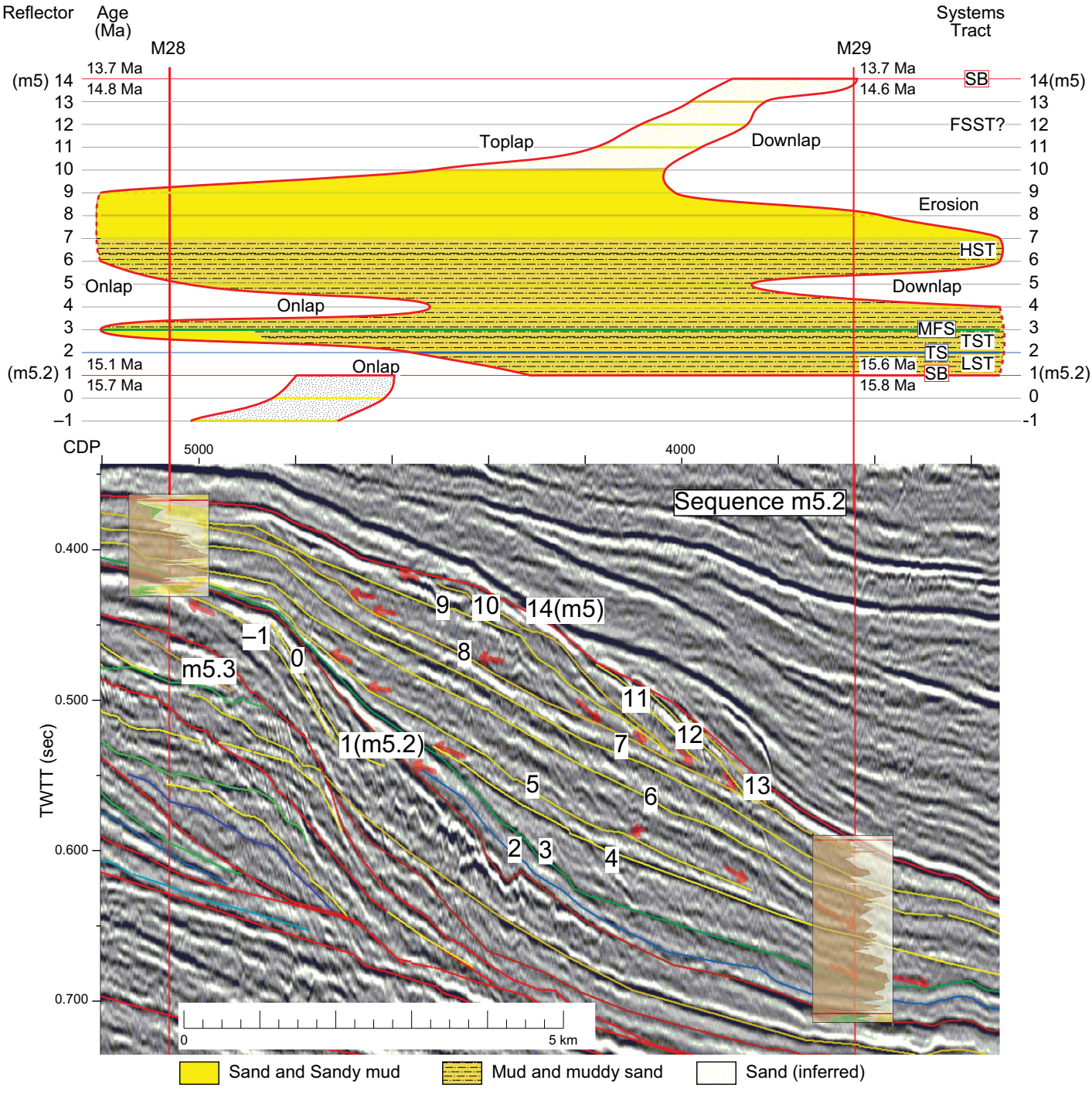

Figure 10. Interpreted seismic profile and Wheeler diagram of sequence m5.2 across the foreset at Integrated Ocean Drilling Program Expedition 313 Site M29, extending to the topset at Site M28. Caption as in Figure 5.

at its thickest point (~140 ms, Fig. 5; 133.59 m, Fig. 4) at Site M27; Sites M28 and M29 sampled sequence m5.8 in offshore prodelta environments on the bottomset.

A prominent, high-amplitude reflector (3 in Fig. 5) onlaps and downlaps the seismic sequence boundary and ties to Site M27 at ~477.52 m composite depth (mcd; Fig. 4). We identify this as the TS at a faint contact zone noted in the core (313-M27–166R-2, 40–56 cm; 477.36–477.52 mcd) based on an uphole change from coarsening upward to fining upward at M27 at the level of this reflector. The LST below this (494.87–477.52 mcd) consists of two upward-coarsening parasequences (arrows indicate fining direction, Fig. 4).

Placement of the MFS is unclear in sequence m5.8 at Site M27 (Fig. 4). The TST fines upward to at least 460 mcd, with clear coarsening beginning above 435 mcd. Lithologic criteria suggest that the MFS occurs in core 158 or 157 where

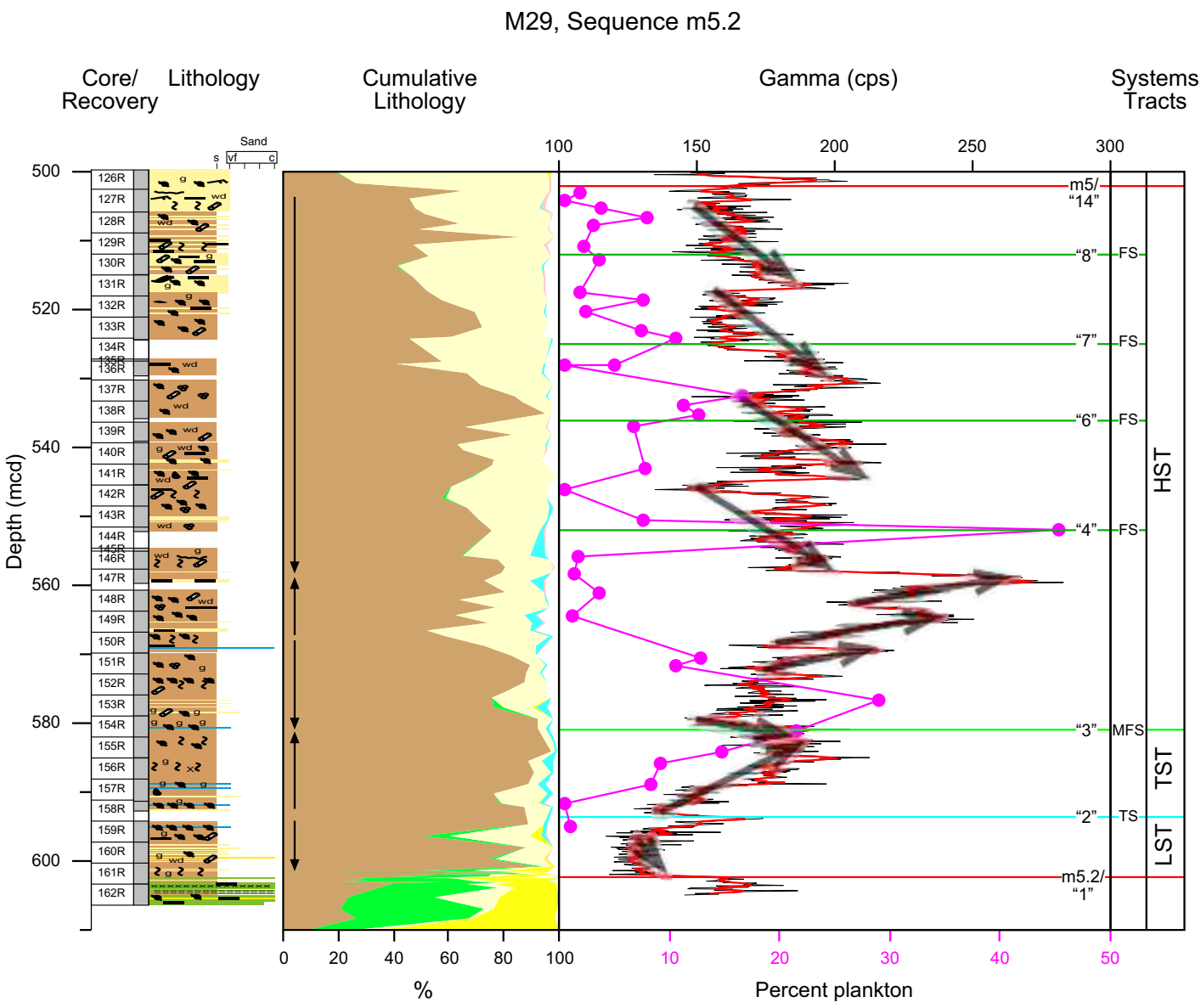

Figure 11. Enlargement of m5.2 sequence in the foreset at Integrated Ocean Drilling Program Expedition 313 Site M29. Lithology and cumulative lithology columns as in Figure 9 (see Fig. 4 caption). Percent plankton of total foraminifera indicated in magenta. The gamma log (thin black line) has been smoothed with a 0.6 m filter (red line). Arrows point in inferred fining direction.

mica, laminations, and percent sand reach a minimum; there is no clear observable surface other than a burrowed interval overlying a concretion (158–1, 30 cm; 451.36 mcd) that may mark the MFS. Benthic foraminifera indicate deepening upward to the deepest paleodepths at 457.78 mcd where planktonic foraminiferal percentages peak at 41%. A major downlap surface (5 in Fig. 5, placed at ~442 mcd in Fig. 4) is traced from Sites M28 and M29 (where extensive downlap is noted), and carried over the rollover. It appears to tie to 442 mcd at Site M27. This major downlap surface is the best seismic candidate for an MFS. However, tracing this surface into the site is unclear and it is possible that the downlap surface correlates deeper (e.g., reflector 4 in Fig. 5). The slight differences in placement based on seismic, lithologic, and benthic foraminiferal criteria illustrate that picking a definitive MFS is not always unequivocal. Our interpretation at Site M27 concludes that the MFS occurs within a zone of maximum flooding from 460 to 435 mcd (see Loutit et al., 1988). Above this zone, the HST progressively coarsens upward to fine sand at ~415 mcd and above that to a blocky, aggradational medium-coarse sand from 400 mcd to the overlying sequence boundary at 361.28 mcd. Seismic profiles show a clear progradation from the seismic MFS (5 in Fig. 5) to reflector 7 and general aggradation above this (Fig. 5).

Both Sites M28 and M29 sampled sequence m5.8 in a bottomset location where the dominant facies is tan clayey silt to silty clay deposited in dysoxic prodelta environments (Mountain et al., 2010; Fig. 4). Above the m5.8 sequence boundary at Site M28 (662.98 mcd), there is a thin basal lag of glauconite sand and overlying glauconitic quartz sand, with rapid fining upwards to ~660 mcd. The major downlap surface reflector 5 correlates at 654 mcd to the contact between a silty clay below and uniform

prodelta clayey silt above, suggesting that this is the deepwater equivalent to the MFS. Benthic foraminifera are absent from the m5.8 sequence at Site M28. At Site M29, glauconitic siltstones deposited in offshore environments overlie the sequence boundary (753.80 mcd). The seismic downlap surface (reflector 5) at Site M29 correlates with an upward change to uniform prodelta clayey silts. Benthic foraminifera indicate paleodepths of 50–80 m immediately above the sequence boundary; paleodepths increase upsection to 75–100 m, and possibly decrease to 50–100 m at the top of the sequence. It is not possible to definitely assign these bottomset deposits below the deepwater equivalent to the MFS at Sites M28 and M29 to the LST or TST based on seismic, lithologic, or benthic foraminiferal criteria, although at least some equivalence to the TST at Site M27 is implied (see correlations in Fig. 4).

Sequence m5.8 appears to be a million-year–scale sequence based on seismic, lithologic, benthic foraminiferal, and age criteria. The Wheeler diagram (Fig. 5, top) also suggests that it is one sequence. The m5.8 sequence is dated as 20.1–19.2 Ma at Site M27 in the foreset and as 20.0–19.5 Ma at Site M28 and 20.2–20.0 Ma at Site M29 in the bottomsets, suggesting that the bottomsets do not record the younger part of the sequence (Fig. 4; Browning et al., 2013). The basal m5.8 sequence boundary correlates with the Miocene oxygen isotope event Mi1aa $\delta^{18}O$ increase based on biostratigraphy and stable isotope stratigraphy (Browning et al., 2013), a relatively minor glacioeustatic lowering (i.e., 0.8‰ increase corresponding to ~40 m lowering). It also correlates with the Burdigalian-1 sequence boundary of ExxonMobil (Snedden and Liu, 2010).

Sequence m5.4 Composite Sequence

Site M28 was designed to sample the thickest part of sequence m5.4 on the foreset, close to the rollover of the overlying m5.3 sequence boundary (Figs. 3, 6, and 7; Supplemental Figs. 4[4] and 5[5]; Mountain et al., 2010). On line 529 (Fig. 7), the sequence is bracketed by two high-amplitude, prominent reflectors (m5.4 and m5.3; Figs. 3 and 7) associated with onlaps, downlaps (e.g., reflector 5 in Fig. 7), toplaps, and erosional truncations. These are clear seismic sequence boundaries and they have been traced through the seismic grid (Monteverde et al., 2008; Monteverde, 2008).

Reflections 0 to 3 (Fig. 7) underlying the m5.4 seismic sequence boundary are part of the underlying m5.45 sequence (Fig. 7) and may represent an FSST because they appear to step down, although this may merely be a result of truncation of the HST by the m5.4 sequence boundary. Tracing sequence boundary m5.4 and distinguishing it from the possible FSST is clear if criteria of onlap, downlap, erosional truncation, and toplap are followed.

At the million-year scale, sequence m5.4 is interpreted seismically to consist of (1) a thick LST (123 m) evidenced by weak aggradation to reflector m5.34 (7) and strong progradation above m5.34 to the major downlap surface marked by reflector m5.32 (14) (Figs. 3 and 7), and (2) a 30-m-thick progradational to aggradational HST above the m5.32 downlap surface to the overlying m5.3 sequence boundary. There apparently is no seismic evidence for an intervening TST (Fig. 7). However, the million-year-scale sequence m5.4 (spanning ca. 17.7–16.7 Ma at Site M28; Fig. 6) is a composite sequence (sensu Mitchum and Van Wagoner, 1991; Neal and Abreu, 2009; Flint et al., 2011) that can be parsed into three sequences, m5.4–1, m5.34, and 5.33 (we use the term 5.4–1 to differentiate the higher frequency sequence, but both the million year and higher frequency sequences share the same basal sequence boundary, reflector m5.4). Coring and logging reveal that this sequence has a very complex internal structure, and integration of seismic, lithologic, foraminiferal, and log criteria justify recognizing three distinct sequences within the m5.4 composite sequence.

Lithologic and benthic foraminiferal patterns are key criteria to resolving this composite sequence (Fig. 6). Two coarsening-upward parasequences separated by a thin fining-upward succession occur at Site M28 between the m5.4 sequence boundary (512.33 mcd) and reflector 5 (Figs. 6 and 7). This 11-m-thick interval is interpreted as the LST. Reflector 5 (Fig. 7) correlates to a level where there is a change from coarsening to fining upward in the cores at 501 mcd, and is thus interpreted as a TS (Fig. 6). The LST is overlain by an abruptly fining-upward succession from 501 to 494 mcd that is interpreted as the TST (Fig. 6). Benthic foraminiferal biofacies, percent plankton, and grain size changes all indicate deepening in the TST above 501 mcd to an MFS associated with reflector 6 at 494 mcd (Fig. 6). The section then coarsens upsection in the HST to a major reflector (7, m5.34) at 479 mcd (Figs. 6 and 7).

We interpret m5.34 as a seismic and core sequence boundary. It shows onlap by reflectors 8 and 10, downlap by reflectors 8 and 9, and erosionally truncates the m5.4 sequence boundary (Fig. 4). We traced m5.34 to adjacent profiles in the seismic grid and found evidence that it is a seismic sequence boundary using criteria of onlap, downlap, erosional truncation, and toplap.

Lithologic, foraminiferal, and log data can be used to recognize systems tracts within the m5.34 sequence (Fig. 6). At Site M28, there is a coarsening-upward succession immediately above m5.34 (479 mcd) to ~475 mcd that we interpret as an LST (Fig. 6). The latter is approximately the level of reflector 8 (467 mcd) that downlaps and onlaps m5.34 (Fig. 7). Thus, we interpret reflector 8 as a TS, and suggest its correlation at 475 mcd, 8 m below its predicted depth. Subsequent fining upward occurs from ~475 to ~468 mcd (Fig. 6) in the lower part of the TST. It is difficult to pick the MFS for the m5.34 sequence because the section lacks foraminifera below 430 mcd (presumably due to dissolution), the cumulative lithology is complicated by the interlaminations of sand and silt that obscure trends, and the dynamic range of the gamma-log values (Fig. 6) is dampened by larger variations above and below.

Examining parasequences within the m5.34 sequence at Site M28 allows us to identify the MFS. Expanding the gamma log (Fig. 8) shows values increasing from 470 to 449 mcd (punctuated by decreases at ~466, ~460, and ~454 mcd), and then generally decreasing to 417 mcd, where there is an abrupt shift to low gamma-log values (Fig. 6). We interpret this as four progressively deeper parasequences, with the MFS identified by gamma logs at 449 mcd in a coring gap (Fig. 8); lithologic descriptions similarly note the change from fining to coarsening upward at ~445 mcd (Mountain et al., 2010). A downlap surface (reflector 10, Fig. 7) correlates to Site M28 at ~449 mcd, suggesting that this is the MFS. The sequence coarsens upsection in the HST (445–405 mcd) and benthic foraminifera show evidence for shallowing. Decreasing gamma-log values upsection are consistent with coarsening upward, with 5 progressively shallower parasequences indicated by FS at 442, 435, 432, and 427 mcd (Fig. 8).

[4]Supplemental Figure 4. Enlargement of Figure 6. If you are viewing the PDF of this paper or reading it offline, please visit http://dx.doi.org/10.1130/GES00884.S4 or the full-text article on www.gsapubs.org to view Supplemental Figure 4.

[5]Supplemental Figure 5. Uninterpreted (top) and interpreted (bottom) seismic profile *Oc270* Line 529 highlighting the m5.4 composite sequence. Scales are two-way travel-time (TWTT) in seconds and Common Depth Point. Approximate scale in km is given. Vertical red line indicates location of Site M28. Arrows indicate reflector termination. Red are sequence boundaries, blue are transgressive surfaces, green are maximum flooding surfaces, and shades of yellow are other reflectors. Numbers (0 to 21) are arbitrary designations. If you are viewing the PDF of this paper or reading it offline, please visit http://dx.doi.org/10.1130/GES00884.S5 or the full-text article on www.gsapubs.org to view Supplemental Figure 5.

The parasequences in the TST have thicker fining-upward successions overlain by thinner coarsening-upward successions; in the HST, the pattern is reversed, with thinner fining-upward and thicker coarsening-upward successions.

We tentatively interpret reflector m5.33 as a sequence boundary based on onlap and downlap, and due to the major downlap onto reflector m5.32 (reflector 14), we interpret it as an MFS. The absence of intersecting profiles with clear seismic definition means that loop correlations cannot confirm that m5.33 is a seismic sequence boundary. At Site M28, candidate sequence boundary m5.33 correlates to ~405 mcd in an interval of poor recovery. A change at 393 mcd from a coarsening- to a fining-upward succession marks the change from the LST to a TST and placement of the TS at this level. Reflector m5.32 (reflector 14) correlates to 391 mcd at a large gamma kick associated with a change from fining upward to coarsening upward. Benthic foraminiferal evidence and percent planktonic foraminiferal evidence indicate a maximum paleowater depth within this sequence at the level of this MFS. Coarsening associated with progradation continues from 391 mcd upward to 380 mcd, ending with blocky, aggradational sands at the top. The HST above m5.32 at Site M27 is seismically composed of a series of inclined and downstepping reflectors possibly reflecting an FSST or erosional truncation of the HST clinoforms (Fig. 7).

The age-distance Wheeler diagram clearly illustrates the nature of the composite sequence (Fig. 7). The m5.4–1 sequence steps seaward of the previous m5.45 sequence and then steps landward, but is truncated by the overlying m5.34 sequence, with its HST poorly developed. The m5.34 sequence steps farther seaward than the underlying sequence, and then fully landward in the TST, with a better developed HST. The m5.33 sequence steps farther seaward than m5.4–1 and m5.34, with the best developed HST. Overall m5.4–1 and m5.34 are progradational and m5.33 is aggradational to progradational. We note that lower resolution seismic data and/or poor core recovery would most likely have failed to resolve each of these embedded sequences, and the composite m5.4 sequence would have been interpreted as a thick LST (which in reality is the m5.4–1 and m5.34 sequences and LST of m5.33) with a thinner, highly downlapping HST (which is the HST of the m5.33 sequence).

Site M27 sampled the million-year-scale m5.4 sequence at a topset where it is composed of the m5.34 and m5.33 sequences; the m5.4–1 sequence appears to have been eroded at this location (Fig. 7). The m5.34 sequence consists of a thin transgressive lag above the sequence boundary (295.01 mcd) and a thin TST that fines up to an MFS at 288 mcd. The HST coarsens upsection to the m5.33 sequence boundary (271.23 mcd) and is thus 17 m thick. In the m5.33 sequence, a possible thin TST (271.23–265 mcd) is overlain by an especially mud-rich interval with the deepest paleodepth within this sequence, based on benthic foraminifera, strongly suggesting an MFS at ~265 mcd. A thin (~9 m) HST caps the sequence, ending at the overlying m5.3 sequence boundary (preferred placement at 256.19 mcd, although it could be placed at 249.75 mcd; see Miller et al., 2013). Thus, both sequences 5.34 and m5.33 at Site M27 consist of thin TST and moderately thick HST on the topsets. Based on lithology the m5.33 sequence is finer grained at Site M27 than at the more basinward Site M28. Furthermore, water depth estimates for m5.33 are deeper at Site M27 than at M28. We interpret this as indicating that the m5.33 sequence at Site M27 represents only the upper TST and lower HST and that this same interval is expressed as a hiatus (0.7 m.y.) at Site M28.

Composite sequence m5.4 was sampled at Site M29 in a bottomset setting and dated as 17.7–17.6 Ma (Figs. 6 and 12). This suggests that the bottomset portion correlates with the m5.4–1 sequence, although the age resolution allows correlation to the m5.34 sequence. Seismic correlations suggest that the m5.34 sequence is present at Site M29. The bottomset consists of fairly uniform silts with transported glauconite sandstone beds.

Age estimates for the m5.4-m5.34-m5.33 composite sequence are consistent with more than one sequence. Sr isotope age estimates show a mean linear fit of 17.7–16.7 Ma for the m5.4 composite sequence at Site M28. In Browning et al. (2013), the ages of m5.4–1 (17.75–17.67 Ma), m5.34 (17.60–17.40 Ma), and m5.33 (16.70–16.60 Ma) were estimated. Maximum theoretical resolution for this portion of the Sr isotope curve is ±0.3 m.y. (see discussion in Browning et al., 2013). Given this, the mean age of m5.33 (16.65 Ma) is statistically different from the older two ages, although the mean ages of m5.34 (17.5 Ma) and m5.4–1 (17.65 Ma) are not statistically different. Thus, it is clear that the age control requires at least two sequences with a significant hiatus separating them.

The basal sequence boundary of the composite sequence m5.4 (ca. 17.7 Ma) correlates with the Mi1b $\delta^{18}O$ increase (17.7 Ma; Browning et al., 2013), a relatively minor glacioeustatic lowering (i.e., ~0.8‰ increase corresponding to ~40 m lowering). It also correlates with the Burdigalian-4 sequence boundary of ExxonMobil (Snedden and Liu, 2010). The correlation of the m5.34 and m5.33 sequence boundaries to $\delta^{18}O$ variations is uncertain due to the lack of high-resolution data in this interval, although the hiatus between m5.4 and m5.34 (17.4–16.7 Ma) may correlate with a 400-k.y.-scale increase ca. 16.8 Ma. Deposition of the m5.33 sequence correlates with an interval of peak sea level in the early Miocene climatic optimum (Fig. 12).

Sequence m5.2

The basal m5.2 sequence boundary is defined by onlap, downlap, erosional truncation, and toplap on line 529 (Figs. 3, 9, and 10; Supplemental Figs. 6[6] and 7[7]) and elsewhere in the available seismic grid. A possible FSST occurs below the sequence boundary in the m5.3 sequence (reflectors –1, 0; cdp 4900–4950, Fig. 10), although this could be due to truncation of the HST of the underlying sequence by m5.2. The m5.2 basal sequence boundary correlates to 602.25 mcd at Site M29, where it was sampled in the lower foreset (Fig. 9). Reflector 2 in Figure 10 onlaps and downlaps the m5.2 sequence boundary and correlates to 593 mcd at Site M29; this is immediately above the top of a coarsening-upward succession at ~593 mcd, suggesting that the TS is at 593 mcd and that the LST is ~9 m thick. The overlying TST (~593–581 mcd) fines upsection and is capped by a prominent downlap surface (3) at ~581 mcd interpreted as the MFS. High planktonic foraminiferal abundances at 576.76 (Fig. 11) support placement of the MFS near reflector 3. A thick (79 m) HST above this contains several FS within it (Figs. 9, 10, and 11), consistent with the presence of at least 4 downlap surfaces noted on the seismic profile (Fig. 10), reflectors 3 (the MFS), 4, 5, and 8. Downlap is not obvious on seismic reflectors 6 and 7. However, we note that reflectors 4, 6, 7, and 8 correlate with flooding surfaces noted in the gamma logs and lithology as mud peaks (Figs. 9 and 11);

[6]Supplemental Figure 6. Enlargement of Figure 9. If you are viewing the PDF of this paper or reading it offline, please visit http://dx.doi.org/10.1130/GES00884.S6 or the full-text article on www.gsapubs.org to view Supplemental Figure 6.

[7]Supplemental Figure 7. Uninterpreted (top) and interpreted (bottom) seismic profile *Oc270* Line 529 highlighting the m5.2 sequence. Scales are two-way travel-time (TWTT) in seconds and Common Depth Point. Approximate scale in km is given. Vertical red line indicates location of Site M29. Arrows indicate reflector terminations. Red are sequence boundaries, blue are transgressive surfaces, green are maximum flooding surfaces, and shades of yellow are other reflectors. Numbers (–1 to 14) are arbitrary designations. If you are viewing the PDF of this paper or reading it offline, please visit http://dx.doi.org/10.1130/GES00884.S7 or the full-text article on www.gsapubs.org to view Supplemental Figure 7.

the slight offset in depths (2–4 m) appears to be consistent and due to a minor problem with the velocity-depth function. Onlap onto reflectors 3 and 8 suggests that they may be sequence boundaries and that m5.2 is also a composite sequence. We lack the data to make this interpretation, although erosional surfaces noted in the cores at 577.89 and 573.66 mcd may be a higher frequency sequence boundary and TS. It is possible that the downstepping associated with reflectors 9–13 represents an FSST (Fig. 10), although erosional truncation of this section could also explain apparent downstepping.

At Site M28, sequence m5.2 was sampled immediately landward of the rollover where it consists of a thin TST and a thick HST with three FS indicated by mud and gamma-log peaks (Fig. 9) and seismic downlap surfaces 6, 7, and 8-9 (Fig. 10). At Site M27, sequence m5.2 consists of a thin (~6 m) TST and thin HST sampled on a topset (Fig. 9).

The age-distance Wheeler diagram (Fig. 10) shows that the m5.2 sequence is predominantly aggradational, although immediately above reflector 8 it becomes strongly progradational to reflector 10, where it apparently steps seaward and downward as a possible FSST (reflectors 10–13). Foreset beds of m5.2 at Site M29 (where the sequence is thickest) are ca. 15.6–14.6 Ma (Fig. 12). Rollover (Site M28) and topset (Site M27) strata are 15.1–14.8 Ma, suggesting nondeposition of the LST and lower TST and the upper HST (Fig. 9). The basal m5.2 sequence boundary (15.6 Ma) appears to be younger than the major Mi2 $\delta^{18}O$ increase (16.3 Ma) and older than the major Mi2a (14.6 Ma) (both >1‰, >50 m eustatic fall). It may be associated with a smaller (0.8‰, ~40 m eustatic fall) 400-k.y.-scale $\delta^{18}O$ increase (Fig. 12), although age control in this interval is less certain and it is possible that it correlates with Mi2a within the age constraints. We suggest it correlates with the Bur5-Lan1 sequence boundary of Exxon-Mobil (16 Ma; Snedden and Liu, 2010).

DISCUSSION

Systems Tracts and Sequence Stratigraphic Models

Our systems tracts interpretations allow us to test sequence stratigraphic models, particularly in the foresets where we recovered lowstand deposits. Drilling through the foresets yields generally thin LST (<18, 11, 4, 12, and 9 m thick for sequences m5.8, m5.4–1, m5.34, m5.33, and m5.2, respectively; Figs. 4, 6, and 9). On the foresets, we also identified thin TST (26, 7, 26, 2, 12 m thicknesses for sequences m5.8, m5.4–1, m5.34, m5.33, and m5.2, respectively). However, thick HST occur on the foresets (90, 15, 44, 30, and 79 m thicknesses for sequences m5.8, m5.4–1, m5.34, m5.33, and m5.2, respectively; Figs. 4, 6, and 9). LST on the foresets consist of one (Fig. 9) to two (Figs. 4 and 6) coarsening-upward parasequences. TS are recognized in foresets by shifts from coarsening-upward successions to fining-upward successions. TST on the foresets record parasequences as overall thick fining-upward (deepening) successions punctuated by thin coarsening-upward (shallowing) parasequences (e.g., Figs. 8 and 11). HST on the foresets reflect the inverse, because thin fine-grained units overlie thicker coarsening-upward parasequences (Figs. 8 and 11).

Topsets consist of shallow-water deposits (shoreface to middle neritic) above merged surfaces that represent both TS and sequence boundaries. TST on topsets consist of fining- and deepening-upward successions overlain by coarsening- and shallowing-upward HST.

Bottomsets consist of downslope-transported sands and hemipelagic muds deposited in 75–100 m water depths (Mountain et al., 2010). Facies successions within bottomsets are not discussed here.

FSST are possibly recognized below seismic sequence boundaries below the rollover. Examples are shown on line 529 in sequence m5.45 below sequence m5.4 (Fig. 7), in m5.3 below m5.2 (Fig. 10), and possibly in m6 below m5.8 (Fig. 5). These FSST have not been confirmed on adjacent profiles. Where sampled, these possible FSST appear to consist of blocky sands (Figs. 7 and 10).

Our interpretation of thin LST contrasts with published seismic stratigraphic predictions of thick LST and thin to absent TST. Greenlee et al. (1992) examined widely spaced profiles tied to logs of exploration wells and proposed that Miocene sequences on the New Jersey shelf stratigraphically above our sequence m5 (their "Green" sequence) were dominated by LST. In Monteverde et al. (2008) and Monteverde (2008), thick LST and thick HST for sequences m5.8, m5.4, and m5.2 were also interpreted (Fig. 13). Here we compare these former interpretations with our conclusions that have the benefit of higher resolution and more densely spaced seismic data, along with core and log integration. Interpretations based on seismic profiles alone (Fig. 13, bottom) tend to overestimate the extent and thickness of LST while underestimating TST (Fig. 13). Possible reasons why LST are overestimated include the following. (1) TS are difficult to distinguish seismically; this explains the different interpretations of sequence m5.8 (Fig. 13). (2) Composite sequences can contain stacked higher frequency sequences that are difficult to distinguish from LST; this explains the different interpretations of sequence m5.4 (see following for further discussion). (3) Sequences contain multiple downlap surfaces, the stratigraphically lowest being the MFS; this explains the different interpretations of sequence m5.2.

We find no evidence for sequence boundaries expressed as correlative conformities in the shallow (<120 m paleodepth) sequences sampled by Expedition 313. We show on the age-distance Wheeler diagrams that in the foresets, where sequences are supposed to be most complete, there is evidence of erosion (Figs. 5, 7, and 10) and hiatuses. For example, we note hiatuses of 0.6, 0.2, 0.7, and 0.2 m.y. associated with the m5.8, m5.4-1, m5.33, and m5.2 sequence boundaries in the foresets, respectively. Longer hiatuses occur on the bottomset, presumably due to erosion and sediment bypass associated with downslope processes (Mountain et al., 2010). Only the higher frequency sequence boundary m5.34 has no discernible hiatus and may reflect continuous deposition (Fig. 7). There are several other sequence boundaries with no discernible time gaps with the resolution available (0.25–0.5 m.y.) (Browning et al., 2013); however, there is still core evidence of erosion in the cores associated with sequence boundaries, even in bottomsets.

If the correlative conformity exists, it is on the continental slope, but even there, hiatuses are associated with sequence boundaries and downslope transport (Miller et al., 1996). ODP Site 904 (Mountain et al., 1996) drilled Miocene sequences on the slope (1123 m water depth) where a long hiatus (15.6–13.6 Ma) encompassing the m5.2 sequence described here was reported (Miller et al., 1996), plus short hiatuses (16.9–16.3 Ma, ca. 22–21 Ma) and inferred continuous sedimentation from 21 to 16.9 Ma encompassing sequences m5.8 to m5.6 described here. However, sedimentation rates in the interval of inferred continuity on the slope are low (~10 m/m.y.) and continuous sedimentation is unproven. Reevaluation of correlations to Site 904 and the chronology there will be the subject of future work. In Mountain et al. (2007), Pleistocene reflectors were traced to the New Jersey continental slope ODP Site 1073 (650.9 m water depth), where continuity is demonstrated by correlation to $\delta^{18}O$ records on the Milankovitch scale; two sequence boundaries in particular, p2 and p3, correlate with marine isotope chrons 8–9 (300 ka) and 11–12 (424 ka), respectively, and exhibit no obvious hiatuses. In contrast, Aubry (1993) found no evidence of continuity for Miocene slope sequences in the Desoto Canyon area (west Florida). Studies of a corehole on the continental slope (300 m) in

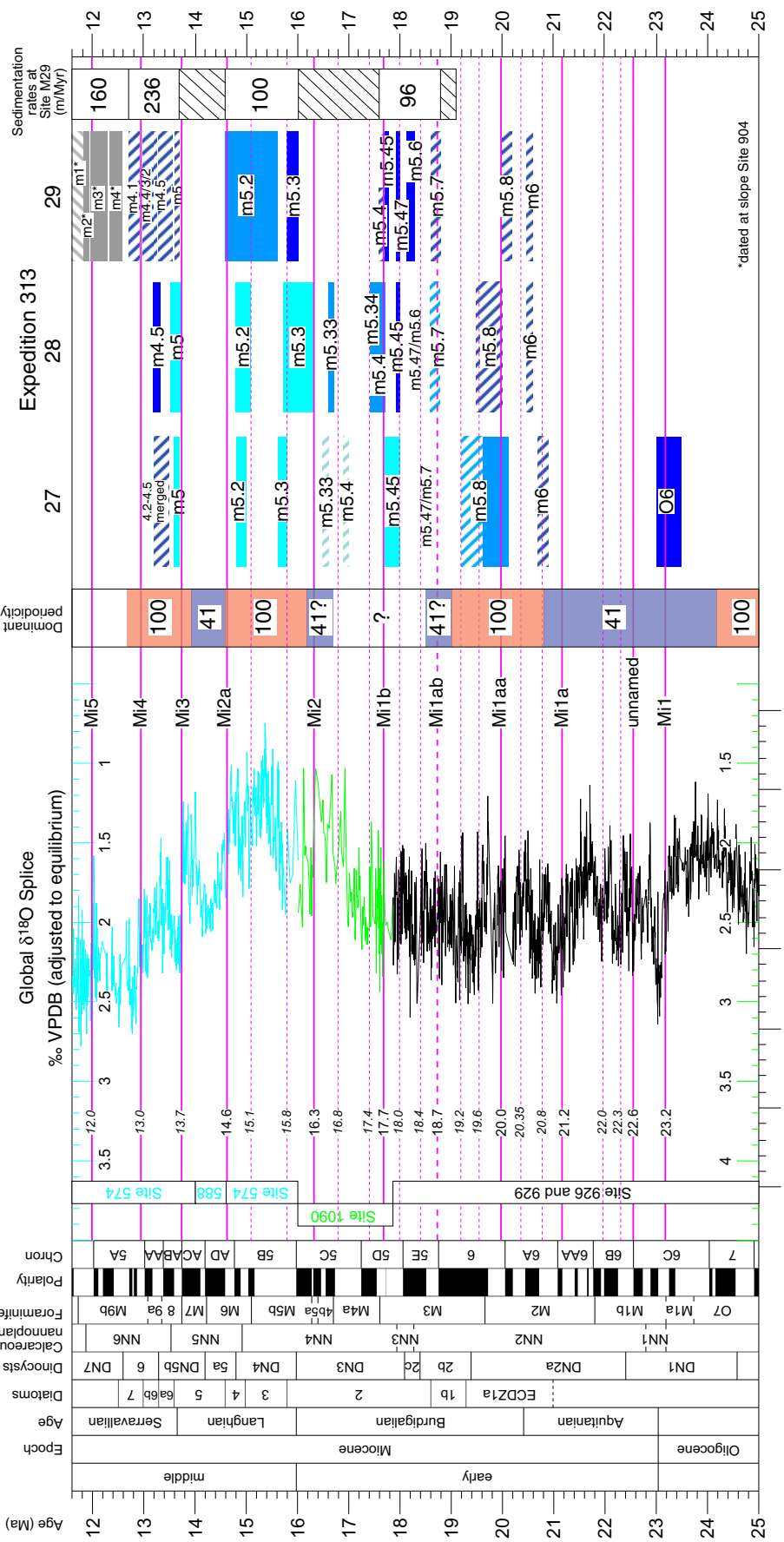

Figure 12. Ages of sequences m6 to m5 and correlation to deep-sea $\delta^{18}O$ records (modified after Browning et al., 2013). Pink horizontal indicates inflections in $\delta^{18}O$ increases. Colored blocks show time periods represented by Integrated Ocean Drilling Program Expedition 313 coreholes compared to the global oxygen isotope record (VPDB—Vienna Peedee belemnite). Mi prefix is Miocene oxygen isotope event. Time scale of Gradstein et al. (2004). Coreholes arranged from updip on left to downdip on right. Different colored blocks are used to show where the site is located with respect to the clinothem and the time represented by a given sequence: light blue (topset), medium blue (foreset), and dark (bottomset). Cross-hachures indicate less certain age tuned to better dated records at other sites. Benthic foraminiferal oxygen isotope records from Site 574 (blue), Site 588 (blue), Site 1090 (green), and Site 926 (black). The dominant periods found in deep-sea $\delta^{18}O$ records are summarized after Pälike et al. (2006) and Holbourn et al. (2007), and are indicated by orange (eccentricity dominated, 100 and 405 k.y.) versus violet (tilt dominated, 41 k.y.) See Browning et al. (2013) for citations.

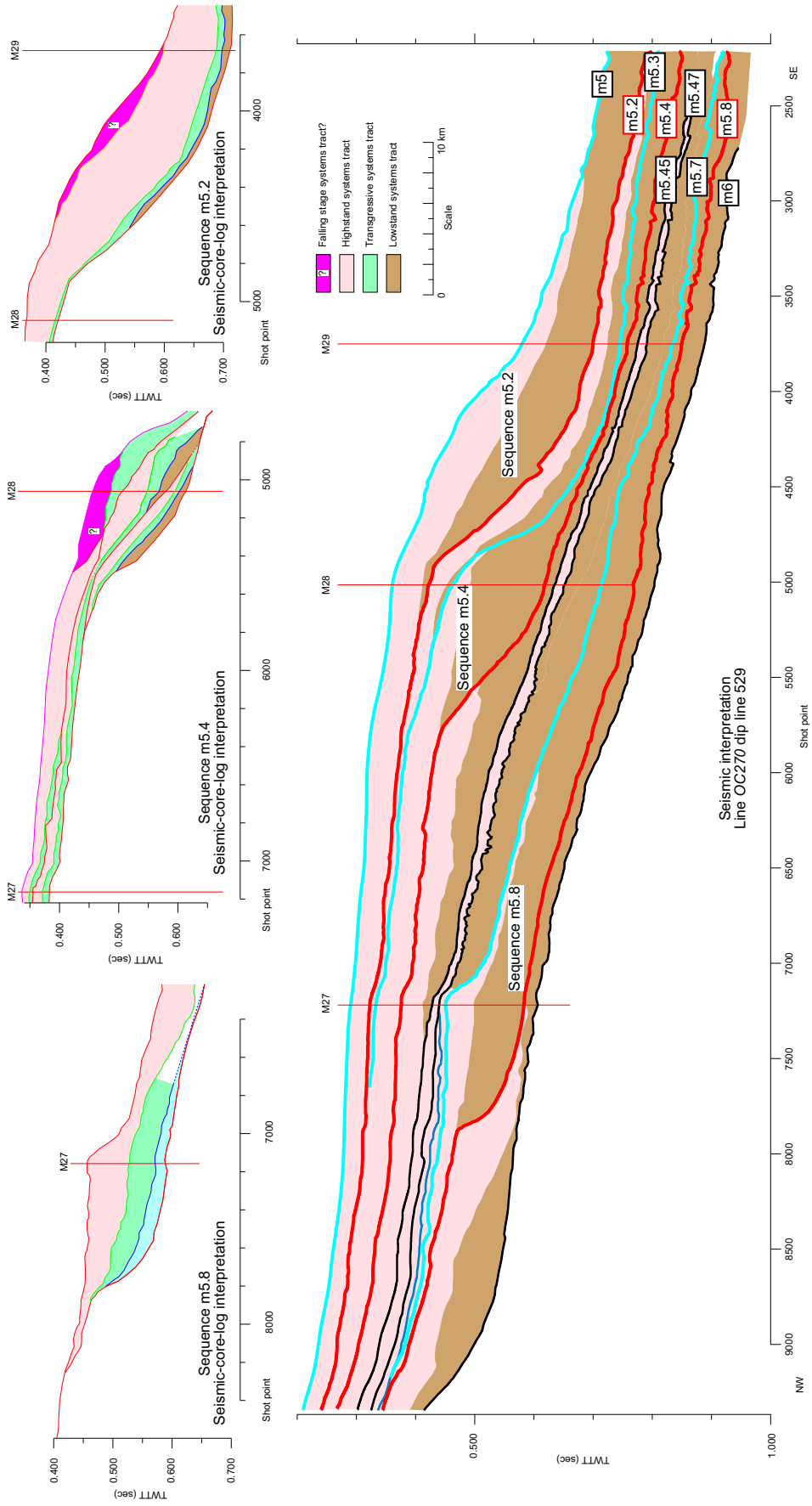

Figure 13. Comparison of systems tracts predicted from seismic profiles (below; Monteverde et al., 2008; Monteverde, 2008) with the seismic-core-log interpretations developed here (top 3 panels). Sections are in two-way travel-time (TWTT) in second (s) versus cdp (common depth point); approximate scale (in km) is shown. Locations of sites are shown by vertical red lines and approximate depth is indicated using a velocity-depth function. Basal sequence boundaries discussed here are in red.

the Gulf of Lion (Western Mediterranean Sea) show very expanded glacial sections and condensed interglacial sections (Sierro et al., 2009), contradicting previous seismic interpretations of reflectors as correlative conformities corresponding to the low sea levels caused by glacial buildup. We conclude that the existence of a correlative conformity is unproven and should not be considered a cornerstone of sequence stratigraphy.

Higher Frequency Sequences and Sequence Hierarchy

We agree with many studies that recognize that sequences on the million-year scale can be the composite of smaller scale sequences (e.g., Mitchum and Van Wagoner, 1991; Neal and Abreu, 2009; Flint et al., 2011). Here we show that sequence m5.4 is a composite sequence comprising three higher frequency sequences. The composite m5.4 sequence shows a change from a thick aggradation-progradation succession to extensively progradational succession across a major downlap surface (m5.32); on the million-year scale, this would be interpreted as dominantly LST, no TST, and a thin HST. However, we show that the LST are actually very thin within the three sequences that comprise composite sequence m5.4. This is illustrated by Figure 13, which shows the million-year-scale interpretation based on seismic interpretations (bottom panel) versus the integrated interpretation that requires three sequences (top panel). We suspect that there is additional detail still to be detected within sequence m5.2 as well, and it may also be composite, but available data are insufficient to evaluate this. This underscores the long-recognized fact that the ability to resolve sequences depends on seismic resolution. Sequences finer than the million year scale can be usually be resolved only in regions with high accommodation and sediment supply (e.g., Abdulah and Anderson, 1994), with very high resolution seismic data, or from detailed outcrop mapping over large areas (e.g., DiCelma et al., 2011; Flint et al., 2011).

There have been two approaches to classifying sequence hierarchy. The Exxon approach has been to recognize hierarchical orders of sequences, with first order (10^8 yr scale) due to tectonism, second order (10^7 yr) and third order (10^6 yr scale) due to various possible processes, and higher order scales due to Milankovitch forcing on the 405 k.y., 100 k.y., 41 k.y., 23 k.y., and 19 k.y. scales (Vail et al., 1977; Mitchum and Van Wagoner, 1991). Schlager (2004) suggested that sequences and systems tracts are scale-invariant fractal features and that they do not follow hierarchical orders. Boulila et al. (2011) noted that icehouse (Oligocene to Holocene) million-year-scale $\delta^{18}O$ variations were paced by the 1.2 m.y. tilt cycle; they suggested that sequences appear to follow the 1.2 m.y. cycle due to glacioeustatic forcing. In contrast, greenhouse (Cretaceous–Eocene) sequences seem to be paced by the 2.4 m.y. eccentricity cycle, although this has not been demonstrated unequivocally.

Oxygen isotope studies show that although million-year-scale ice volume variability was dominated by the 1.2 m.y. tilt cycle, there were numerous changes in the dominant higher frequency pacemaker in the early to middle Miocene, from eccentricity (100 and 405 k.y.) dominated to tilt (41 k.y.) dominated benthic foraminiferal $\delta^{18}O$ variations (Pälike et al., 2006; Holbourn et al., 2007). Sequences m5.8 and m5.2 were deposited in a 100 k.y. cycle–dominated world, indicated by wavelet analysis of $\delta^{18}O$ data (Pälike et al., 2006) (Fig. 12). Unfortunately, $\delta^{18}O$ resolution is insufficient at present to document the dominant pacing of the interval from 18.5 to 16.6 Ma, the time encompassing composite sequence m5.4 (Fig. 12). Higher frequency sequences within the m5.4 composite sequence suggest response to the 100 and/or 400 k.y. eccentricity cycles and perhaps even the 23 and 19 k.y. precessional cycles (Fig. 12).

Our chronology is consistent with oxygen isotope studies indicating that early Miocene sequences were paced by 1.2 m.y. tilt and 100 k.y. and 405 k.y. eccentricity cycles (Fig. 12). Sequence m5.8, composite sequence m5.4, and sequence m5.2 have been dated (20.1–19.2, 17.7–16.6, and 15.6–14.6 Ma; Browning et al., 2013) with durations of 0.9, 1.1, and 1 m.y., respectively, close to the 1.2 m.y. predicted by Milankovitch glacioeustatic forcing (Fig. 12). The 3 sequences and hiatuses within the m5.4 composite sequence constrain the duration of the sequences to 400 k.y. or shorter time scales. Our age model suggests durations of ~80, ~200, and ~100 k.y. for the 3 higher frequency sequences m5.4–1, m5.34, and m5.33. However, age control is no better than ±250 k.y., and thus we cannot demonstrate that these sequences were forced by the 100 k.y. or the longer 405 k.y. eccentricity cycle. Nevertheless, log data provide intriguing hints of much higher resolution forcing that may be a response to precessional (23 and 19 k.y.) forcing (Figs. 8 and 11). Flooding surfaces (parasequence boundaries) inferred from the gamma log within the m5.34 sequence (Fig. 8) are ~25 k.y. in duration (i.e., 8 cycles in the 50 m of section shown on the inset representing <200 k.y.), consistent with precession forcing. If precessional forcing occurs, then it should be modulated by eccentricity forcing on the ~100 and 405 k.y. scale.

We suggest that although sequences may appear to be fractal and scale invariant (Schlager, 2004), they are in fact controlled by astronomical forcing with distinct periodicities. Although we lack age control to unequivocally document 1.2 m.y., 405 k.y., or ~100 k.y. periodicities in our sequences, it is clear that glacioeustatic forcing occurred in the early to middle Miocene interval examined here (Fig. 12). Our chronology supports the existence of a 1.2 m.y. beat in early Miocene sequences and is consistent with a response on the 400 or 100 k.y. scale.

Paleodepth of Seismic Stratigraphic Features

Several issues remain to be addressed by Expedition 313 studies, including the influence of paleotopography of the clinothem on deposition (particularly lowstand deposits), paleorelief between the clinoform inflection and the bottomset, and the paleodepth of the rollovers and lowest point of onlap. Benthic foraminifera indicate that the bottomsets were deposited in ~100 m of water or slightly deeper. Sequences on the foresets are typically 150–200 m thick, with topsets as much as 200 ms (~200 m) above the bottomsets. This would imply greater water depth than indicated by benthic foraminifera. However, the role of loading on paleotopography (including two-dimensional effects) must be accounted for (Steckler et al., 1999). For example, two-dimensional backstripping shows that vertical differences in original geometry are muted compared to observed sediment thickness, especially in foresets (Kominz and Pekar, 2001).

We see no evidence for subaerial exposure on the clinothems sampled here (m5.8, m5.4 composite, and m5.2). Several sequences were sampled at the clinoform rollover: (1) m5.7 (which overlies m5.8) at Site M27, where the environments are coarsening-upward shoreface as part of a HST; (2) m5.33 at M28, where the environments are interpreted as shoreface coarsening upward in the LST; and (3) m5.3 (which overlies m5.32) at M28, where the environments are shoreface-offshore transition. Our observations are consistent with the recovery of lagoonal environments at ODP Site 1071 (Austin et al., 1998), 3 km landward of the m0.5 rollover. Together, this suggests that shorelines consistently move as far seaward as clinoform rollovers and that the depositional environment of the point of onlap at the clinoform rollover is nearshore in this area.

We sampled the lowest point of seismic onlap seaward of the rollover (reflector 8) in sequence m5.34 at Site M28 (Figs. 6 and 7). Here, the onlap associated with the LST and

TS is a coarsening-upward offshore (50–75 m) environment. Sequence m5.33 was also sampled near the lowest point of onlap (between the sequence boundary and reflector 13), where it consists of shoreface deposits (Figs. 6 and 7). These observations should prove to be useful in future work.

Back to Basics

Neal and Abreu (2009) eschewed the use of sea-level curves in recognizing systems tracts. Here we do not use relative sea-level curves in our interpretations of systems tracts; rather, we use basic seismic, core, and stratigraphic principles to recognize sequence boundaries, MFS, TS, and facies successions within sequences. We use facies successions and stratal surfaces to subdivide sequences into systems tracts. We focus on fining- and deepening-upward and coarsening- and shallowing-upward trends (Fig. 1) deciphered with lithologic and foraminiferal data that are applicable on topsets and foresets, but less applicable on bottomsets. Our simple predictive model of coarsening and fining trends (Fig. 1) is similar to the accommodation successions method of Neal and Abreu (2009) that focuses on progradational-aggradational-retrogradational patterns observed in seismic profiles (their Fig. 2). These complementary approaches allow objective recognition of systems tracts that are not tied to preconceived notions.

CONCLUSIONS

We show that identification of seismic sequences using classic criteria is robust, allowing objective subdivision into sequences. Seismic sequence boundaries are recognized on topsets, foresets, and bottomsets and can be clearly differentiated from FSST and/or truncated HST and attendant surfaces. MFS can be generally inferred with seismic criteria as a downlap surface, although caution must be exercised in picking the stratigraphically lowest downlap surface as the MFS. We see little evidence for correlative conformities. Distinguishing LST and TST seismically is a challenging task. We show that interpretation of systems tracts requires integration of seismic, core (lithology and foraminifera), and geophysical logs to develop unequivocal interpretations. Sequences embedded within million-year-scale composite sequences can be particularly challenging to interpret using seismic profiles alone. We note that our study area is consistent with preserving hierarchical orders of sequences on the tilt (1.2 m.y.) and eccentricity scales (100 and 405 k.y.).

ACKNOWLEDGMENTS

We thank the drillers and scientists of Integrated Ocean Drilling Program (IODP) Expedition 313 for their enthusiastic collaboration, the Bremen Core Repository for hosting our studies, and C. Lombardi, J. Criscione, and R. Miller for lithologic analyses. Funding was provided by COL/USSP, and samples were provided by the IODP and the International Continental Scientific Drilling Program. We thank B. Bracken and an anonymous reviewer for reviews, M. Kominz for discussions, and V. Abreu for bringing us back to basics.

REFERENCES CITED

Abdulah, K.C., and Anderson, J.B., 1994, Contrasting styles of deltaic deposition and the role of eustasy—Example from the Quaternary deltas of the Texas continental shelf, *in* Application of sequence stratigraphy to oil field development: Hedberg Research Conference Proceedings: Tulsa, Oklahoma, American Association of Petroleum Geologists, p. 1–11.

Aubry, M.-P., 1993, Neogene allostratigraphy and depositional history of the DeSoto Canyon area, northern Gulf of Mexico: Micropaleontology, v. 39, p. 327–366, doi:10.2307/1485855.

Austin, J.A., Christie-Blick, N., Malone, M.J., and others, 1998, Initial Reports, Ocean Drilling Program, Leg 174A: College Station, Texas, Ocean Drilling Program, 324 p.

Boulila, S., Galbrun, B., Miller, K.G., Pekar, S.F., Browning, J.V., Laskar, J., and Wright, J.D., 2011, On the origin of Cenozoic and Mesozoic "third-order" eustatic sequences: Earth-Science Reviews, v. 109, p. 94–112, doi:10.1016/j.earscirev.2011.09.003.

Brown, L.F., and Fisher, W.L., 1977, Seismic-stratigraphic interpretation of depositional systems: Examples from Brazilian rift and pull-apart basins, *in* Payton, C.E., ed., Seismic stratigraphy—Applications to hydrocarbon exploration: American Association of Petroleum Geologists Memoir 26, p. 213–248.

Browning, J.V., Miller, K.G., McLaughlin, P.P., Kominz, M.A., Sugarman, P.J., Monteverde, D., Feigenson, M.D., and Hernàndez, J.C., 2006, Quantification of the effects of eustasy, subsidence, and sediment supply on Miocene sequences, Mid-Atlantic margin of the United States: Geological Society of America Bulletin, v. 118, p. 567–588, doi:10.1130/B25551.1.

Browning, J.V., Miller, K.G., Sugarman, P.J., Kominz, M.A., McLaughlin, P.P., and Kulpecz, A.A., 2008, 100 Myr record of sequences, sedimentary facies and sea-level change from Ocean Drilling Program onshore coreholes, U.S. Mid-Atlantic coastal plain: Basin Research, v. 20, p. 227–248, doi:10.1111/j.1365-2117.2008.00360.x.

Browning, J.V., Miller, K.G., Sugarman, P.J., Barron, J., McCarthy, F.M.G., Kulhanek, D.K., Katz, M.E., and Feigenson, M.D., 2013, Chronology of Eocene–Miocene sequences on the New Jersey shallow shelf: Implications for regional, interregional, and global correlations: Geosphere, doi:10.1130/GES00857.1.

Catuneanu, O., 2006, Principles of sequence stratigraphy: Elsevier, Amsterdam, 375 p.

Catuneanu, O., and 27 others, 2009, Towards the standardization of sequence stratigraphy: Earth-Science Reviews, v. 92, p. 1–33, doi:10.1016/j.earscirev.2008.10.003.

Christie-Blick, N., 1991, Onlap, offlap, and the origin of unconformity-bounded depositional sequences: Marine Geology, v. 97, p. 35–56, doi:10.1016/0025-3227(91)90018-Y.

Christie-Blick, N., and Driscoll, N.W., 1995, Sequence stratigraphy: Annual Review of Earth and Planetary Sciences, v. 23, p. 451–478, doi:10.1146/annurev.ea.23.050195.002315.

Christie-Blick, N., Mountain, G.S., and Miller, K.G., 1988, Sea level history: Science, v. 241, p. 596, doi:10.1126/science.241.4865.596.

Christie-Blick, N., Mountain, G.S., and Miller, K.G., 1990, Seismic stratigraphic record of sea level change, *in* Geophysics Study Committee, Sea-level change: National Research Council Studies in Geophysics: Washington, D.C., National Academy Press, p. 116–140.

Coe, A.L., ed., 2003, The sedimentary record of sea level change: Cambridge, Cambridge University Press, 288 p.

Demarest, J.M., and Kraft, J.C., 1987, Stratigraphic record of Quaternary sea levels: Implications for more ancient strata, *in* Nummedal, D., et al., eds., Sea level fluctuation and coastal evolution: Society of Economic Paleontologists and Mineralogists Special Publication 41, p. 223–239, doi:10.2110/pec.87.41.0223.

DiCelma, C.N., Brunt, R.L., Hodgson, D.M., Flint, S.S., and Kavanagh, J.P., 2011, Spatial and temporal evolution of a Permian submarine slope channel-levee system, Karoo Basin, South Africa: Journal of Sedimentary Research, v. 81, p. 579–599, doi:10.2110/jsr.2011.49.

Embry, A.F., 2009, Practical sequence stratigraphy: Canadian Society of Petroleum Geologists, 81 p., www.cspg.org.

Flint, S.S., Hodgson, D.M., Sprague, A.R., Brunt, R.L., Van der Merwe, W.C., Figueiredo, J., Prélat, A., Box, D., Di Celma, C., and Kavanagh, J.P., 2011, Depositional architecture and sequence stratigraphy of the Karoo basin floor to shelf edge succession, Laingsburg depocentre, South Africa: Marine and Petroleum Geology, v. 28, p. 658–674, doi:10.1016/j.marpetgeo.2010.06.008.

Galloway, W.E., 1989, Genetic stratigraphic sequences in basin analysis I: Architecture and genesis of flooding-surface bounded depositional units: American Association of Petroleum Geologists, Bulletin, v. 73, p. 125–142.

Gradstein, F., and 38 others, 2004, A geologic time scale 2004: Cambridge, Cambridge University Press, 589 p.

Greenlee, S.M., and Moore, T.C., 1988, Recognition and interpretation of depositional sequences and calculation of sea level changes from stratigraphic data—Offshore New Jersey and Alabama Tertiary, *in* Wilgus, C.K., et al., eds., Sea-level changes: An integrated approach: Society of Economic Paleontologists and Mineralogists Special Publication 42, p. 329–353, doi:10.2110/pec.88.01.0329.

Greenlee, S.M., Schroeder, F.W., and Vail, P.R., 1988, Seismic stratigraphic and geohistory analysis of Tertiary strata from the continental shelf off New Jersey—Calculation of eustatic fluctuations from stratigraphic data, *in* Sheridan, R., and Grow, J., eds., The Atlantic continental margin: U.S.: Boulder, Colorado, Geological Society of America, Geology of North America, v. I-2, p. 437–444.

Greenlee, S.M., Devlin, W.J., Miller, K.G., Mountain, G.S., and Flemings, P.B., 1992, Integrated sequence stratigraphy of Neogene deposits, New Jersey continental shelf and slope: Comparison with the Exxon model: Geological Society of America Bulletin, v. 104, p. 1403–1411, doi:10.1130/0016-7606(1992)104<1403:ISSOND>2.3.CO;2.

Hancock, J.M., 1993, Transatlantic correlations in the Campanian-Maastrichtian stages by eustatic changes of sea-level, *in* Hailwood, E.A., and Kidd, R.B., eds., High resolution stratigraphy: Geological Society of London Special Publication 70, p. 241–256, doi:10.1144/GSL.SP.1993.070.01.17.

Hancock, J.M., and Kauffman, E.G., 1979, The great transgressions of the Late Cretaceous: Geological Society of London Journal, v. 136, p. 175–186, doi:10.1144/gsjgs.136.2.0175.

Hathaway, J.C., Poag, C.W., Valentine, P.C., Miller, R.E., Schultz. D.M., Manheim, R.T., Kohout, F.A., Bothner, M.H., and Sangrey, D.A., 1979, U.S. Geological Survey core drilling on the Atlantic shelf: Science, v. 206, p. 515–527.

Heezen, B.C., Tharp, M., and Ewing, M., 1959, The floors of the oceans: I. The North Atlantic: Geological Society of America Special Paper 65, 122 p., doi:10.1130/SPE65-p1.

Holbourn, A.E., Kuhnt, W., Schulz, M., Flores, J.-A., and Andersen, N., 2007, Orbitally-paced climate evolution during the middle Miocene "Monterey" carbon-isotope excursion: Earth and Planetary Science Letters, v. 261, p. 534–550, doi:10.1016/j.epsl.2007.07.026.

Katz, M.E., Browning, J.V., Miller, K.G., Monteverde, D., Mountain, G.S., and Williams, R.H., 2013, Paleobathymetry and sequence stratigraphic interpretations 1 from benthic foraminifera: Insights on New Jersey

shelf architecture, IODP Expedition 313: Geosphere, doi:10.1130/GES00872.1.

Kidwell, S.M., 1989, Stratigraphic condensation of marine transgressive records: Origin of major shell deposits in the Miocene of Maryland: Journal of Geology, v. 97, p. 1–24, doi:10.1086/629278.

Kidwell, S.M., 1991, The stratigraphy of shell concentration, *in* Allison, P.A., and Briggs, D.E.G., eds., Taphonomy: Releasing the data locked in the fossil record: Topics in Geobiology Volume 9: New York, Springer-Verlag, p. 211–290.

Kominz, M.A., and Pekar, S.F., 2001, Oligocene eustasy from two-dimensional sequence stratigraphic backstripping: Geological Society of America Bulletin, v. 113, p. 291–304, doi: 10.1130/0016-7606(2001)113<0291:OEFTDS>2.0.CO;2.

Loutit, T.S., Hardenbol, J., Vail, P.R., and Baum, G.R., 1988, Condensed section: The key to age determination and correlation of continental margin sequences, *in* Wilgus, C.K., et al., eds., Sea-level changes: An integrated approach: Society of Economic Paleontologists and Mineralogists Special Publication 42, p. 183–213, doi:10.2110/pec.88.01.0183.

Miall, A.D., 1991, Stratigraphic sequences and their chronostratigraphic correlation: Journal of Sedimentary Petrology, v. 61, p. 497–505.

Miller, K.G., Mountain, G.S., Leg 150 Shipboard Party, and Members of the New Jersey Coastal Plain Drilling Project, 1996, Drilling and dating New Jersey Oligocene–Miocene sequences: Ice volume, global sea level, and Exxon records: Science, v. 271, p. 1092–1095, doi:10.1126/science.271.5252.1092.

Miller, K.G., Rufolo, S., Sugarman, P.J., Pekar, S.F., Browning, J.V., and Gwynn, D.W., 1997, Early to middle Miocene sequences, systems tracts, and benthic foraminiferal biofacies, New Jersey coastal plain, *in* Miller, K.G., and Snyder, S.W., eds., Proceedings of the Ocean Drilling Program, Scientific Results, Leg 150X: College Station, Texas, Ocean Drilling Program, p. 169 186.

Miller, K.G., Mountain, G.S., Browning, J.V., Kominz, M., Sugarman, P.J., Christie-Blick, N., Katz, M.E., and Wright, J.D., 1998, Cenozoic global sea-level, sequences, and the New Jersey transect: Results from coastal plain and slope drilling: Reviews of Geophysics, v. 36, p. 569–601, doi:10.1029/98RG01624.

Miller, K.G., Browning, J.V., Mountain, G.S., Bassetti, M.A., Monteverde, D., Katz, M.E., Inwood, J., Lofi, J., and Proust, J.-N., 2013, Sequence boundaries are impedance contrasts: Core-seismic-log integration of Oligocene–Miocene sequences, New Jersey shallow shelf: Geosphere, v. 9, doi:10.1130/GES00858.1.

Mitchum, R.M., Jr., and Van Wagoner, J.C., 1991, High-frequency sequences and their stacking patterns; sequence-stratigraphic evidence of high-frequency eustatic cycles: Sedimentary Geology, v. 70, p. 131–160, doi:10.1016/0037-0738(91)90139-5.

Mitchum, R.M., Jr., Vail, P.R., and Thompson, S., III, 1977, Seismic stratigraphy and global changes of sea level; Part 2, The depositional sequence as a basic unit for stratigraphic analysis, *in* Payton, C.E., ed., Seismic stratigraphy; applications to hydrocarbon exploration: American Association of Petroleum Geologists Memoir 26, p. 53–62.

Monteverde, D.H., 2008, Sequence stratigraphic analysis of early and middle Miocene shelf progradation along the New Jersey margin [Ph.D. thesis]: New Brunswick, Rutgers University, 247 p.

Monteverde, D.H., Mountain, G.S., and Miller, K.G., 2008, Early Miocene sequence development across the New Jersey margin: Basin Research, v. 20, p. 249–267, doi: 10.1111/j.1365-2117.2008.00351.x.

Mountain, G., and Monteverde, D., 2012, If you've got the time, we've got the depth: The importance of accurate core-seismic correlation: American Geophysical Union Fall Meeting, abs. PP51B–2111.

Mountain, G.S., Miller, K.G., Blum, P., and Twitchell, D.C., et al., 1996, Proceedings of the Ocean Drilling Program, Scientific results, Volume 150: College Station, Texas, Ocean Drilling Program, 885 p.

Mountain, G.S., Burger, R.L., Delius, H., Fulthorpe, C.S., Austin, J.A., Goldberg, D.S., Steckler, M.S., McHugh, C.M., Miller, K.G., Monteverde, D.H., Orange, D.L., and Pratson, L.F., 2007, The long-term stratigraphic record on continental margins, *in* Nittrouer, C.A., et al., eds., Continental margin sedimentation: From sediment transport to sequence stratigraphy: International Association of Sedimentologists Special Publication 37, p. 381–458.

Mountain, G.S., Proust, J.-N., McInroy, D., and Cotterill, C., and the Expedition 313 Scientists, 2010, Proceedings of the International Ocean Drilling Program, Expedition 313: Tokyo, Integrated Ocean Drilling Program Management International, Inc., doi:10.2204/iodp.proc.313.2010.

Neal, J., and Abreu, V., 2009, Sequence stratigraphy hierarchy and the accommodation succession method: Geology, v. 37, p. 779–782, doi:10.1130/G25722A.1.

Olsson, R.K., Melillo, A.J., and Schreiber, B.L., 1987, Miocene sea level events in the Maryland coastal plain and the offshore Baltimore Canyon trough, *in* Ross, C., and Haman, D., eds., Timing and depositional history of eustatic sequences: Constraints on seismic stratigraphy: Cushman Foundation for Foraminiferal Research Special Publication 24, p. 85–97.

Owens, J.P., and Gohn, G.S., 1985, Depositional history of the Cretaceous series in the U.S. Atlantic coastal plain: Stratigraphy, paleoenvironments, and tectonic controls of sedimentation, *in* Poag, C.W., ed., Geologic evolution of the United States Atlantic margin: New York, Van Nostrand Reinhold, p. 25–86.

Pälike, H., Frazier, J., and Zachos, J.C., 2006, Extended orbitally forced palaeoclimatic records from the equatorial Atlantic Ceara Rise: Quaternary Science Reviews, v. 25, p. 3138–3149, doi:10.1016/j.quascirev.2006.02.011.

Plint, A.G., and Nummedal, D., 2000, The falling stage systems tract: Recognition and importance in sequence stratigraphic analysis, *in* Hunt, D., and Gawthorpe, R.L., eds., Sedimentary responses to forced regression: Geological Society of London Special Publication 172, p. 1–17, doi:10.1144/GSL.SP.2000.172.01.01.

Posamentier, H.W., and Vail, P.R., 1988, Eustatic controls on clastic deposition II—Sequence and systems tract models, *in* Wilgus, C.K., et al., eds., Sea level changes: An integrated approach: Society of Economic Paleontologists and Mineralogists Special Publication 42, p. 125–154, doi:10.2110/pec.88.01.0125.

Posamentier, H.W., Jervey, M.T., and Vail, P.R., 1988, Eustatic controls on clastic deposition I—Conceptual framework, *in* Wilgus, C.K., et al., eds., Sea level changes: An integrated approach: Society of Economic Paleontologists and Mineralogists Special Publication 42, p. 109–124, doi:10.2110/pec.88.01.0109.

Posamentier, H.W., Allen, G.P., James, D.P., and Tesson, M., 1992, Forced regressions in a sequence stratigraphic framework: Concepts, examples, and exploration significance: American Association of Petroleum Geologists Bulletin, v. 76, p. 1687–1709.

Poulsen, C.J., Flemings, P.B., Robinson, R.A.J., and Metzger, J.M., 1998, Three-dimensional stratigraphic evolution of the Miocene Baltimore Canyon region: Implications for eustatic interpretations and the systems tract model: Geological Society of America Bulletin, v. 110, p. 1105–1122, doi:10.1130/0016-7606(1998)110<1105:TDSEOT>2.3.CO;2.

Proust, J.N., Mahieux, G., and Tessier, B., 2001, Field and seismic images of sharp-based shoreface deposits: Implications for sequence stratigraphic analysis: Journal of Sedimentary Research, v. 71, p. 944–957, doi: 10.1306/041601710944.

Rabineau, M., Berné, S., Aslanian, D., Olivet, J.-L., Joseph, P., Guillocheau, F., Bourillet, J.-F., Ledrezen, E., and Granjeon, D., 2005, Sedimentary sequences in the Gulf of Lions: A record of 100,000 years climatic cycles: Marine and Petroleum Geology, v. 22, p. 775–804, doi:10.1016/j.marpetgeo.2005.03.010.

Schlager, W., 2004, Fractal nature of stratigraphic sequences: Geology, v. 32, p. 185–188, doi:10.1130/G20253.1.

Schlee, J.S., 1981, Seismic stratigraphy of Baltimore Canyon Trough: American Association of Petroleum Geologists Bulletin, v. 65, p. 26–53.

Sierro, F.J., and 14 others, 2009, Phase relationship between sea-level and abrupt climate change: Quaternary Science Reviews, v. 28, p. 2867–2881, doi:10.1016/j.quascirev.2009.07.019.

Snedden, J.W., and Liu, C., 2010, A compilation of Phanerozoic sea-level change, coastal onlaps and recommended sequence designations: American Association of Petroleum Geologists Search and Discovery Article 40594, www.searchanddiscovery.com.

Steckler, M. S., Mountain, G. S., Miller, K.G., and Christie-Blick, N., 1999, Reconstruction of Tertiary progradation and clinoform development on the New Jersey passive margin by 2-D backstripping: Marine Geology, v. 154, p. 399–420.

Sugarman, P.J., Miller, K.G., Owens, J.P., and Feigenson, M.D., 1993, Strontium-isotope and sequence stratigraphy of the Miocene Kirkwood Formation, southern New Jersey: Geological Society of America Bulletin, v. 105, p. 423–436, doi:10.1130/0016-7606(1993)105<0423:SIASSO>2.3.CO;2.

Trincardi, F., and Correggiari, A., 2000, Quaternary forced-regression deposits in the Adriatic Basin and the record of composite sea-level cycles, *in* Hunt, D., and Gawthorpe, R., eds., Sedimentary responses to forced regressions: Geological Society of London Special Publication 172, p. 245–269, doi:10.1144/GSL.SP.2000.172.01.12.

Vail, P.R., 1987, Seismic stratigraphy interpretation using sequence stratigraphy: Part 1. Seismic stratigraphy interpretation procedure, *in* Bally A.W., ed., Atlas of seismic stratigraphy: American Association of Petroleum Geologists Studies in Geology 27, p. 1–10.

Vail, P.R., Mitchum, R.M., Jr., and Thompson, S., III, 1977, Seismic stratigraphy and global changes of sea level; Part 4, Global cycles of relative changes of sea level, *in* Payton, C.E., ed., Seismic stratigraphy; applications to hydrocarbon exploration: American Association of Petroleum Geologists Memoir 26, p. 83–97.

Van Wagoner, J.C., Mitchum, R.M., Jr., Posamentier, H.W., and Vail, P.R., 1987, Seismic stratigraphy interpretation using sequence stratigraphy: Part 2, Key definitions of sequence stratigraphy, *in* Bally A.W., ed., Atlas of seismic stratigraphy: American Association of Petroleum Geologists Studies in Geology 27, p. 11–14.

Van Wagoner, J.C., Posamentier, H.W., Mitchum, R.M., Vail, P.R., Sarg, J.F., Loutit, T.S., and Hardenbol, J., 1988, An overview of the fundamentals of sequence stratigraphy and key definitions, *in* Wilgus, C.K., et al., eds., Sea-level changes: An integrated approach: Society of Economic Paleontologists and Mineralogists Special Publication 42, p. 39–45, doi:10.2110/pec.88.01.0039.

Van Wagoner, J.C., Mitchum, R.M., Campion, K.M., and Rahmanian, V.D., 1990, Siliciclastic sequence stratigraphy in well logs, cores, and outcrops: Concepts for high-resolution correlation of time and facies: American Association of Petroleum Geologists Methods in Exploration Series 7, 55 p.

Wheeler, H.E., 1958, Time stratigraphy: American Association of Petroleum Geologists Bulletin, v. 42, p. 1047–1063.